Strain Segregation between Ductile and Brittle Stratigraphy -- Characterizing the Sand Wash Fault System, Uinta Basin, Utah

Riley Brinkerhoff[1], John McBride[2], Sam Hudson[2], Douglas A. Sprinkel[3], Ron Harris[2], Kevin Rey[2], and Eric Tingey[2]

Search and Discovery Article #11363 (2022)**
Posted September 2, 2022

*Adapted from extended abstract based on oral presentation given at 2022 AAPG Rocky Mountain Section Meeting, Denver Colorado, July 24-27, 2022
 DOI:10.1306/11363Brinkerhoff2022

[1]Wasatch Energy Management, 3319 N University Ave., Suite 200, Provo, Utah 84604, (riley.brinkerhoff@gmail.com)
[2]Department of Geological Sciences, Brigham Young University, Provo, Utah 84602, (john_mcbride@byu.edu), (sam.hudson@byu.edu), (rharris@byu.edu), (kd7kmp@gmail.com), (eric.tingey@byu.edu)
[3]Aztec GeoSolutions, 3260 N 1350 W, Pleasant View, Utah 84414, (sprinkel@aztecageo.com)

Abstract

The Sand Wash fault zone is a segmented and discontinuous fault system that strikes northwest to southeast in the central part of the Uinta Basin. It is approximately 34 kilometers long with an uncommonly wide damage zone, typically 100 to 200 meters wide. Due to recent, rapid, and large-scale incision by the Green River and its tributaries, the Sand-Wash fault zone is well exposed in several closely spaced canyons. These canyon exposures allow mapping of the lateral relationships through panoramic photographs and surface kinematic descriptions.

Most movement on the Sand Wash fault zone occurred in the late Eocene, but minor, more recent movement likely occurred. Evidence for fault timing includes strata-bound, syndepositional movement which occurred during Lake Uinta time (55 to 43 Ma BP) resulting in debris flows, slump blocks, and small (>150 meters diameter) sag basins filled with poorly organized sediments. After lithification, elongate grabens formed with up to 33.5 meters of horizontal extension. Two styles of deformation are present. Brittle rocks, such as sandstone and limestone beds, are intensely fractured and faulted, whereas clay-rich and organic-rich rocks are largely unfractured and unfaulted, with variably folded beds that have experienced some layer-parallel slip. Laterally, deformation is distributed up to 100 meters from the fault core, which is uncommonly large for faults with short lengths and little displacement. Vertically, displacement is concentrated in brittle sandstone and carbonate beds and rare in clay- and hydrocarbon-rich units, such as the Mahogany oil-shale zone of the Eocene Green River Formation. The Mahogany oil-shale zone mostly displays ductile flow (granular flow) commonly forming small décollements between overlying and underlying units. Vertical displacement on separate fault segments is generally less than 5 meters and decreases down section, dying out completely around the top of the Mahogany oil-shale zone.

In this presentation we show evidence for syndepositional deformation along the Sand Wash fault zone, strain partitioning along décollement surfaces, fault surfaces that experience multiple deformational phases, pop-up blocks, and graben development. We also show that deformation

on the fault zone is related to extension above a neutral surface of a larger fold. This larger fold is associated with a basement-rooted fault zone that moved during Laramide tectonism with the reactivation of the Uncompahgre uplift. The Sand Wash fault zone appears to have many similarities to the larger, and more deeply buried, Duchesne fault zone 25 kilometers to the north, and the more deeply eroded Cedar Ridge fault zone located 30 kilometers to the south. The high-resolution fault model, developed herein, is thus a good proxy for other complex fault zones in the Uinta Basin. Our model will be useful to oil and gas operators as they develop horizontal wells across this and other complex fault zones in the basin.

References:

Aslan, A., Karlstrom, K.E., Kirby, E., Heizler, M.T., Granger, D.E., Feathers, J.K., Hanson, P.R., and Mahan, S.A., 2019, Resolving time-space histories of Late Cenozoic bedrock incision along the Upper Colorado River, USA: Geomorphology, v. 347, p. 1–26, doi: https://doi.org/10.1016/j.geomorph.2019.106855.

Bader, J.W., 2008, Structural and tectonic evolution of the Cherokee Ridge arch, south-central Wyoming—implications for recurring strike-slip along the Cheyenne belt suture zone: Rocky Mountain Geology, v. 43, no. 1, p. 23–40.

Bader, J.W., 2009, Structural and tectonic evolution of the Douglas Creek arch, the Douglas Creek fault zone, and environs, northwestern Colorado, and northeastern Utah—implications for petroleum accumulation in the Piceance and Uinta Basins: Rocky Mountain Geology, v. 44, no. 2, p.121–145.

Birgenheier, L.P., and Vanden Berg, M.D., 2011, Core-based integrated sedimentologic, stratigraphic, and geochemical analysis of the oil shale bearing Green River Formation, Uinta Basin, Utah: U.S. Department of Energy, National Energy Technology Laboratory, Topical Report, 19 p.

Boden, T., and Tripp, B.T., 2012, Gilsonite veins of the Uinta Basin, Utah: Utah Geological Survey Special Study 141, 48 p., ISBN 978-155791-856-7.

Bradley, W.H., 1931, Origin and microfossils of the oil shale of the Green River Formation of Colorado and Utah: U.S. Geological Survey Professional Paper 168, 58 p.

Brinkerhoff, R., 2019, Characterizing outcrop growth faults, slump blocks, mud volcanoes and other sedimentary deformation features for use as reservoir analogues for observed features in targeted reservoirs in the Green River Formation, Uinta Basin, Utah [abs.]: American Association of Petroleum Geologists, Rocky Mountain Section Meeting, Search and Discovery Article #51623.

Brinkerhoff, R., and Millard, M., 2019, Using pore system characterization to subdivide the burgeoning Uteland Butte play, Green River Formation, Uinta Basin, Utah [abs.]: American Association of Petroleum Geologists, Rocky Mountain Section Meeting, Search and Discovery Article #11272.

Brinkerhoff, R., and Sprinkel, D.A., 2021, Uinta enigma—the Duchesne fault zone and its impact on the development of the Uinta Basin: Rocky Mountain Association of Geologists, The Outcrop, v. 70, no. 3, p. 16–30.

Cashion, W.B., 1967, Geology and fuel resources of the Green River Formation, southeastern Uinta Basin, Utah and Colorado: U.S. Geological Survey Professional Paper 548, 48 p.

Davis, S.J., Mix, H.T., Weigand, B.A., Carroll, A.R., and Chamberlain, C.P, 2010, Synorogenic evolution of large-scale drainage patterns—isotope paleohydrology of sequential Laramide basins: American Journal of Science, v. 309, p. 549–602.

Dickinson, W.R., Lawton, T.F., and Inman, K.F., 1986, Sandstone detrital modes, central Utah foreland region—stratigraphic record of Cretaceous-Paleogene tectonic evolution: Journal of Sedimentary Petrology, v. 56, no. 2, p. 276–293.

Eckels, M.T., Suek, D.H., Harrison, D.H., and Harrison, P.J., 2004, North Hill Creek 3-D seismic exploration project: Ute Indian Tribe, Uintah & Ouray Reservation, Uintah County: U.S Department of Energy, Final Technical Report, 26 p.

Ford, G.L., Pyles, D.R., and Dechesne, M., 2016, Stratigraphic architecture of a fluvial-lacustrine basin-fill succession at Desolation Canyon, Uinta Basin, Utah—reference to Walthers' Law and implications for the petroleum industry: The Mountain Geologist, v. 53, no. 1, p. 5–28.

Fouch, T.D., 1976, Revision of the lower part of the Tertiary system in the central and western Uinta Basin, Utah: U.S. Geological Survey Bulletin 1405-C, p. C1–C7.

Fouch, T.D., Cashion, W.B., Ryder, R.T., and Campbell, J.A., 1976, Field guide to lacustrine and related nonmarine depositional environments in Tertiary rocks, Uinta Basin, Utah, in Epis, R.C., and Weimer, R.J., editors, Professional contributions of Colorado School of Mines-studies in Colorado field geology, Number 8: Colorado School of Mines, p. 358–385.

Fouch, T.D., Nuccio, V.F., Anders, D.E., Rice, D.D., Pitman, J.K., and Mast, R.F., 1994a, Green River (!) petroleum system, Uinta Basin, Utah, U.S.A., *in* Magoon, L.B., and Dow, W.G., editors, The petroleum system— from source to trap: American Association of Petroleum Geologists Memoir 60, p. 399–421.

Fouch, T.D., Wandrey, C.J., Taylor, D.J., Butler, C.B., Miller, J.J., Prensky, S.E., Boone, L.E., Schmoker, J.W., Crovelli, R.A., Beeman, 1994b, Oil and Gas Resources of U.S. Naval Oil Shale Reserves 1 and 3, Colorado, and Reserve 2, Utah: Open-File Report 94-427, U.S. Department of Energy Contract No. DE-AT21-93-MC30141, https://doi.org/10.3133/ofr94427.

Grabowski, G.J., Jr., and Peaver, D.R., 1985, Sedimentology and petrology of profundal lacustrine sediments, Mahogany zone of the Green River Formation, Piceance Creek Basin, northwest Colorado, *in* Crevello, P.D., and Harris, P.M., editors, Deep-water carbonates—buildups, turbidites, debris flows and chalk: Society for Sedimentary Geology (SEPM) Core Workshop 6, p. 386–430.

Grout, M.A., and Verbeek, E.R., 1998, Tectonic and paleostress significance of the regional joint network of the central Paradox Basin, Utah and Colorado: U.S. Geological Survey Bulletin 2158, p.151–166.

Howe, J., and Klinger, R., 2021, Evidence for Quaternary activity on the Duchesne-Pleasant Valley fault, Uinta Basin, Utah: Seismological Society of America Seismological Research Letters, v. 92, no. 2B, p. 1335, doi: https://doi.org/10.1785-/0220210025.

Johnson, R.C., 1985, Early Cenozoic history of the Uinta and Piceance Creek Basins, Utah and Colorado, with special reference to the development of Eocene Lake Uinta, *in* Flores R.M., and Kaplan, S.S., editors, Cenozoic paleogeography of the west-central United States: Society for Sedimentary Geology (SEPM), Rocky Mountain Section, Rocky Mountain Paleogeography Symposium 3, p. 247–276, online, http://archives.datapages.com/ data/rocky_sepm/data/023/023001/247_rocky_mount230247.htm.

Johnson, R.C., and Finn, T.M., 1986, Cretaceous through Holocene history of the Douglas Creek arch, Colorado and Utah, *in* Stone, D.S., editor, New interpretations of northwest Colorado geology: Rocky Mountain Association of Geologists Guidebook, p. 77–95.

Karlstrom, K.E., Crow, R., Crossey, L.J., Coblentz, D., and Van Wijk, J.W., 2008, Model for tectonically driven incision of the younger than 6 Ma Grand Canyon: Geology, v. 36, no. 11, p. 835, doi: 10.1130/g25032a.1.

Keighley, D., 2013, Outcrop chemostratigraphic correlation of the upper Green River Formation in the Uinta Basin, Utah—Mahogany oil shale zone to the Uinta Formation: Utah Geological Survey Miscellaneous Publication 13-1, p. 30.

Keighley, D., Töro, B., Vanden Berg, M.D., and Pratt, B.R., 2015, Deformation within the Mahogany oil shale zone of the Green River Formation at Sand Wash, eastern Utah, USA, *in* Vanden Berg, M.D., Ressetar, R., and Birgenheier, L.P., editors, Geology of Utah's Uinta Basin and Uinta Mountains: Utah Geological Association Publication 44, p. 423–438.

Marshak, S., Nelson, W.J., and McBride, J.H., 2003, Phanerzoic strike-slip faulting in the continental interior platform of the United States: examples from the Laramide Orogen, Midcontinent, and Ancestral Rocky Mountains, *from*: Storti, F., Holdsworth, R.E. and Salvani, F. (eds) *Intraplate Strike-Slip Deformation Belts.* Geological Society, London, Special Publications, 210, 159-184, 0305-8719/03/$15.

Mederos, S., Tikoff, B., and Bankey, V., 2005, Geometry, timing, and continuity of the Rock Springs uplift, Wyoming, and Douglas Creek arch, Colorado—implications for uplift mechanisms in the Rocky Mountain foreland, U.S.A.: Rocky Mountain Geology, v. 40, p. 167–191.

Mews, K., Mustafa, A.M., and Barati, Rh., 2019, A review of brittleness index correlations for unconventional tight and ultra-tight reservoirs: Geosciences, v. 9, 10.3390/geosciences9070319.

Morgan, C.D., 2003, Geologic guide and road logs of the Willow Creek, Indian, Soldier Creek, Nine Mile, Gate, and Desolation Canyons, Uinta Basin, Utah: Utah Geological Survey Open-File Report 407, 74 p., https://geology.utah.gov/resources/ energy/oil-gas/green-river-formation-project/.

Morgan, C.D., McClure, K.P., Bereskin, S.R., and McPherson, M., 2002, A preliminary discussion of fault styles in the southwest Uinta Basin, Utah [abs.]: American Association of Petroleum Geologists, Rocky Mountain Section Meeting Program with Abstracts, https://geology.utah.gov/resources/energy/oil-gas/green-river-formationproject/.

Osmond, J.C., 1965, Geologic history of the Uinta basin, Utah: American Association of Petroleum Geologists Bulletin, v. 49, n. 11, p. 1957-1973.

Pederson, J., Karlstrom, K., Sharp, W., and McIntosh, W., 2002, Differential incision of the Grand Canyon related to Quaternary faulting—constraints from U-series and Ar/Ar dating: Geology, v. 30, no. 8, p. 739–742.

Remy, R., 1992, Stratigraphy of the Eocene part of the Green River Formation in the south- central part of the Uinta Basin, Utah: U.S. Geological Survey Bulletin B 1787-BB, p. BB1–BB69.

Smith, M.E., Carroll, A.R., and Singer, B.S., 2008, Synoptic reconstruction of a major ancient lake system—Eocene Green River Formation, western United States: Geological Society of America Bulletin, v. 120, no. 1/2, p. 54–84, doi: 10.1130/B26073.1.

Sprinkel, D.A., 2009, Interim Geologic Map of the Seep Ridge 30' x 60' quadrangle: Utah Geological Survey, Utah Geological Survey Open-File Report 549DM, 3 plates.

Sprinkel, D.A., 2014, The Uinta Mountains—a tale of two geographies and more: Utah Geological Survey, Survey Notes, v. 46, no. 3, p. 1–4.

Sprinkel, D.A., 2018, Mysteries of the Uinta Mountains—commonly asked questions and answers: Utah Geological Survey, Survey Notes, v. 50, no. 3, p. 1–3.

Stone, D.S., 1977, Tectonic history of the Uncompahgre uplift, *in* Veal, H.K. editor, Rocky exploration frontiers of the central and southern Rockies: Rocky Mountain Association of Geologists Guidebook, p. 23–30.

Töro, B., and Pratt, B.R., 2015, Characteristics and implications of sedimentary deformation features in the Green River Formation (Eocene) in Utah and Colorado, *in* Vanden Berg, M.D., Ressetar, R., and Birgenheier, L.P., editors, Geology of Utah's Uinta Basin and Uinta Mountains: Utah Geological Association Publication 44, p. 371– 422.

Verbeek, E.R., and Grout, M.A., 1993, Geometry and structural evolution of gilsonite dikes in the eastern Uinta Basin, Utah: U.S. Geological Survey Bulletin 1787-HH, 42 p., 1 plate.

Wawrzyniec, T.F., Geissman, J.W., Melker, M.D., and Hubbard, M., 2002, Dextral shear along the eastern margin of the Colorado Plateau—a kinematic link between Laramide contraction and Rio Grande rifting (Ca. 75–13 Ma): Journal of Geology, v. 110, p. 305–324.

STRAIN SEGREGATION BETWEEN DUCTILE AND BRITTLE STRATIGRAPHY—CHARACTERIZING THE SAND WASH FAULT SYSTEM, UINTA BASIN, UTAH

Riley Brinkerhoff [1] (riley.brinkerhoff@gmail.com)
John McBride[2] (john_mcbride@byu.edu)
Sam Hudson[2] (sam.hudson@byu.edu)
Douglas A. Sprinkel[3] (sprinkel@aztecageo.com)
Ron Harris[2] (rharris@byu.edu)
Kevin Rey[2] (kd7kmp@gmail.com)
Eric Tingey[2] (eric.tingey@byu.edu)

1. Wasatch Energy Management, 3319 N University Ave., Suite 200, Provo, Utah 84604
2. Department of Geological Sciences, Brigham Young University, Provo, Utah 84602
3. Aztec GeoSolutions, 3260 N 1350 W, Pleasant View, Utah 84414

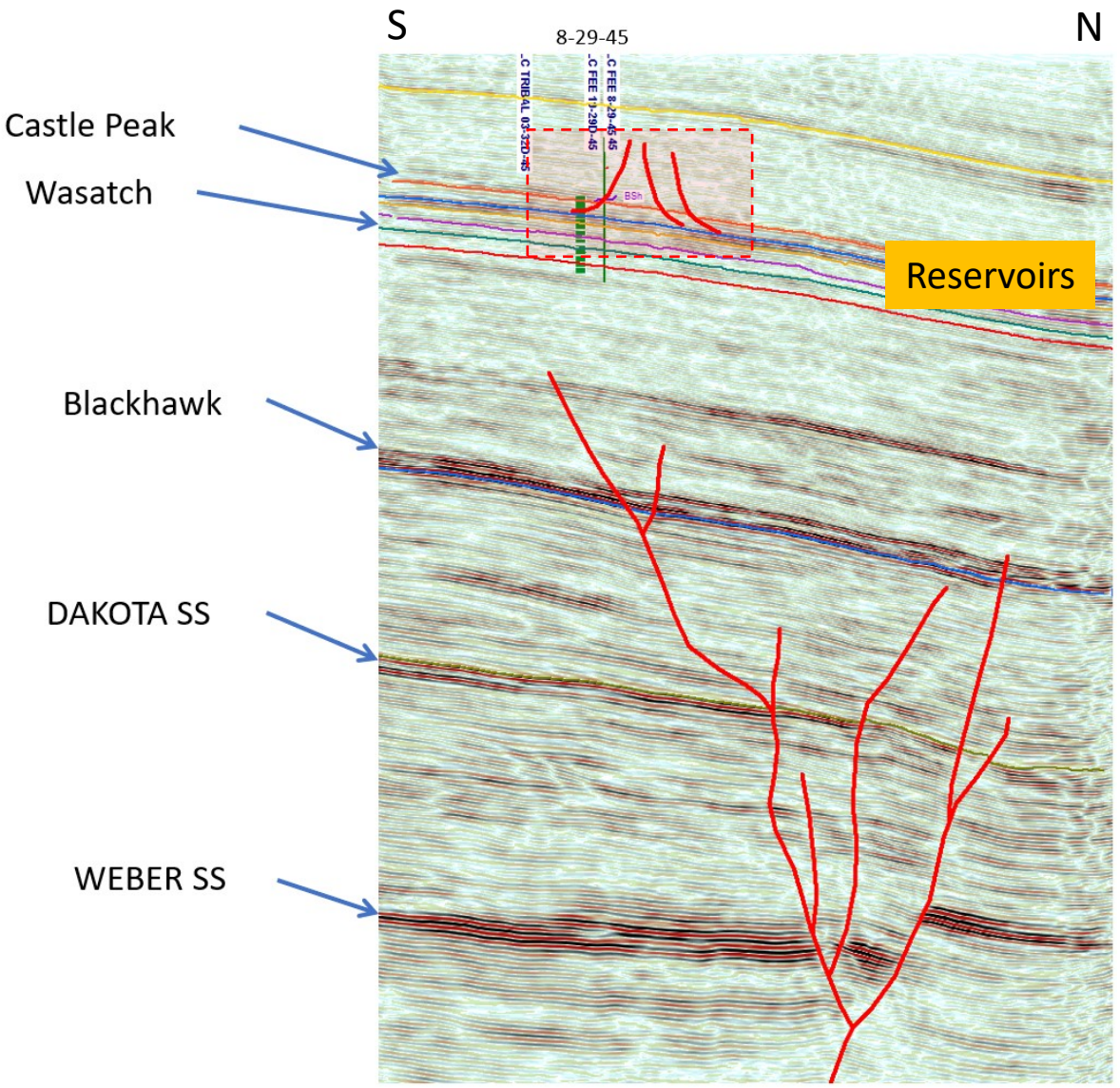

Modified from: Wide-Azimuth 3D Seismic Data Integrated with Geologic Information from Open-Hole Logs Unlocks the Secrets of a Naturally Fractured Trap in the Western Uinta Basin, Utah; W. Korenkiewicz and J. Pyle; 2014 RMS-AAPG Conference, Denver, CO

Problem

- Across the Uinta Basin, poorly understood faults appear to impact oil and gas production
  - Seismic example from the oil-productive Duchesne fault zone
- Near these fault wells encounter highly variable pressures, water zones and far traveled oil
- The genesis and character of the faults needs to be understood

Objective

Provide

- Characterization and descriptions of the superbly exposed Sand Wash Fault System in the study area by integrating
  - Outcrop fault and fracture mapping
  - Photogrammetry
  - Rheology analysis
- A deformation model that explains the variable faulting and fracturing

Location

- The Uinta Basin within northeastern Utah
  - The Sand Wash fault zone (SWFZ) in red in the center of the basin
- The SWFZ is south of the main oil and gas fields in the basin
  - The SWFZ trends northwest-southeast
  - Like other fault zones in the southern Uinta Basin

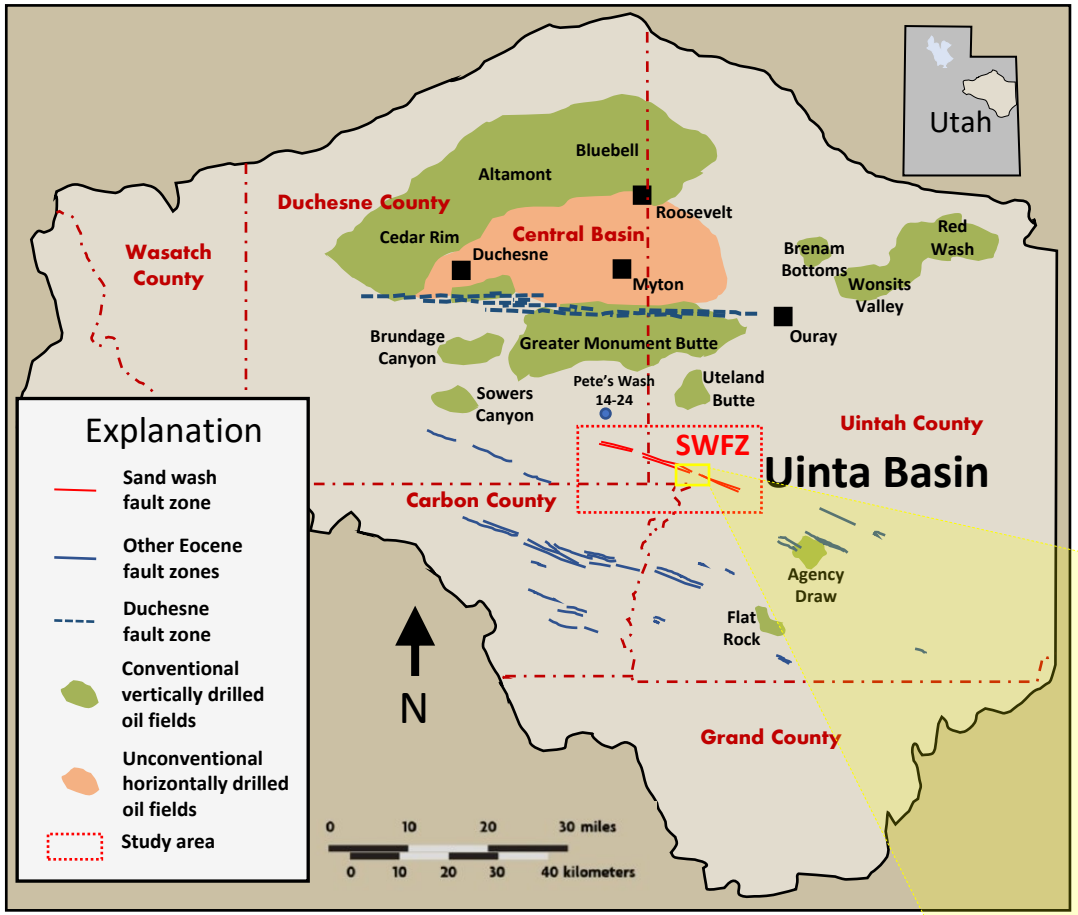

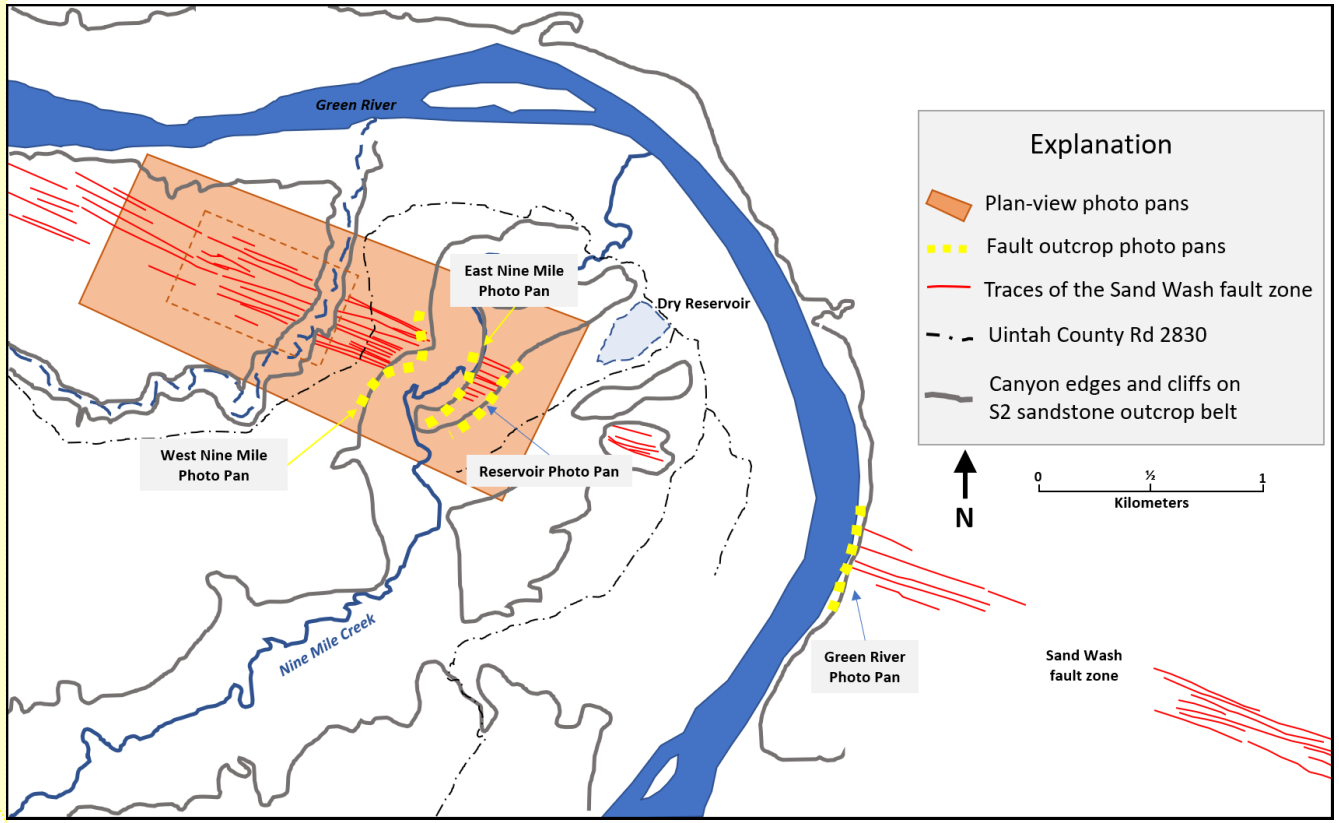

- The study area showing the relation of the fault traces to the photo pans
- The canyon edges are shown because the best exposures of the fault zone and involved stratigraphy are visible there

What is the Sand Wash Fault Zone?

- The SWFZ is a segmented and discontinuous fault system that strikes northwest to southeast in the central part of the Uinta Basin
- It is approximately 34 kilometers long with an uncommonly wide damage zone for such a low-throw fault system
  - Typically, 100 to 200 meters wide

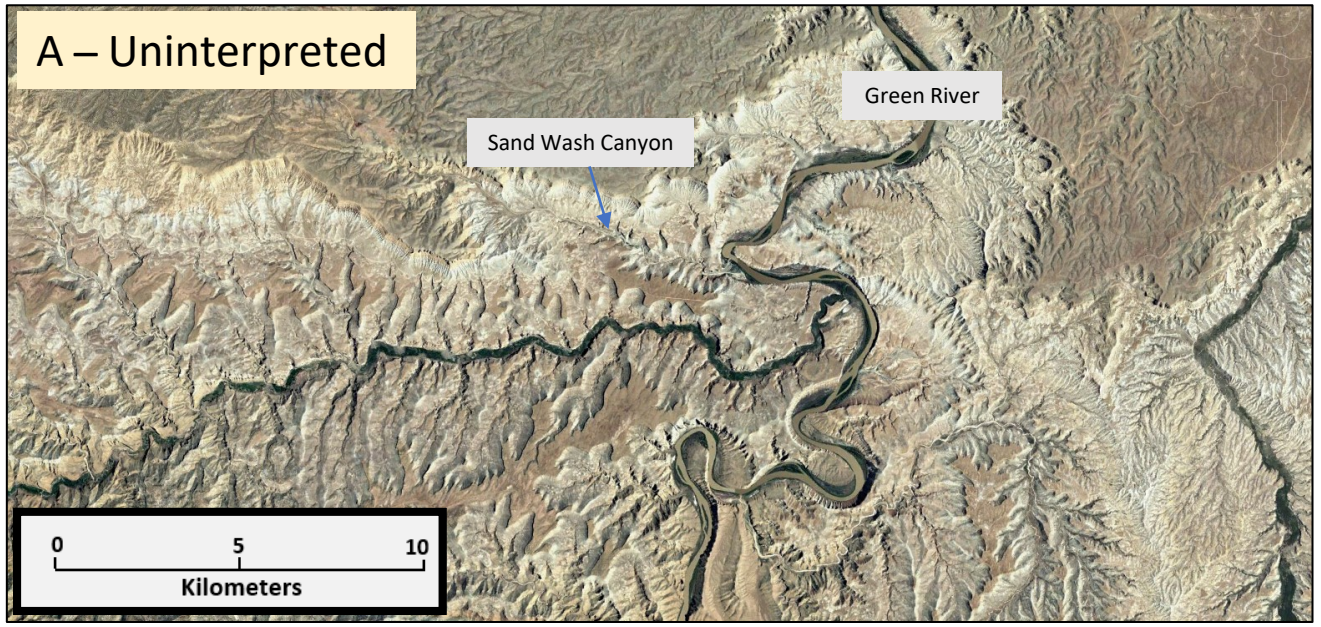

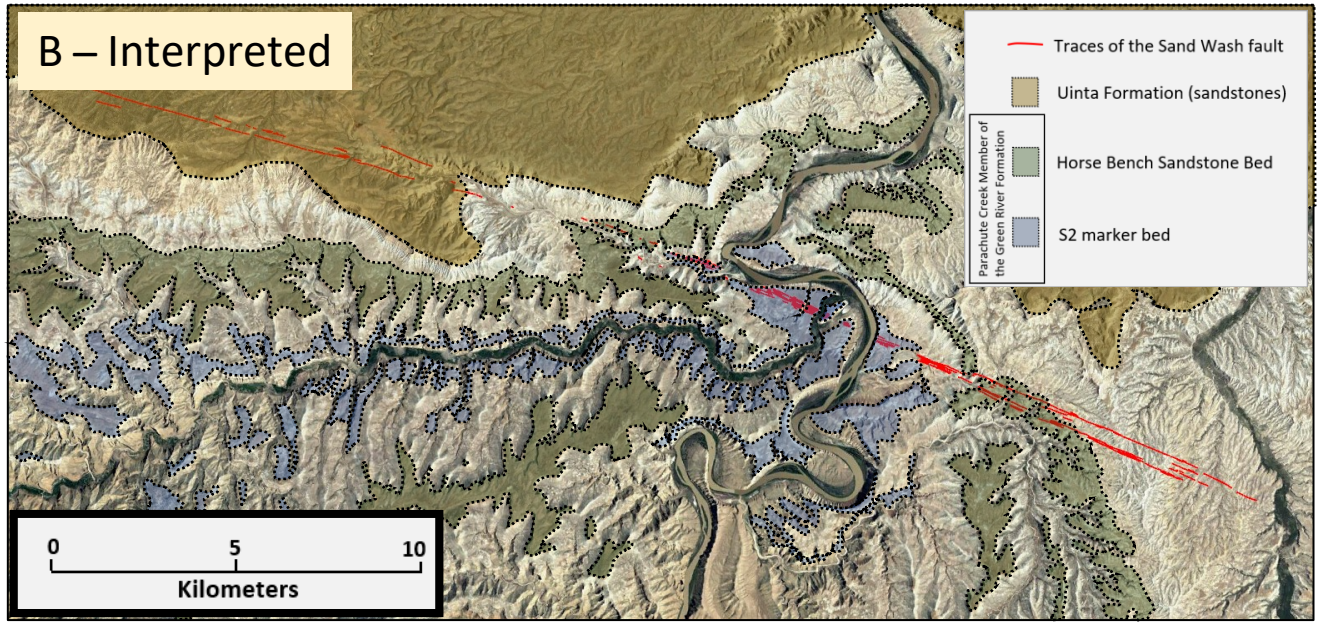

What is the Sand Wash Fault Zone?

The Sand Wash fault zone cuts perpendicularly through the outcrop, creating a beautiful exposure of:

- S2 marker bed having been extended 33.25 meters
  - Breaking into three foundered grabens
  - Complex mix of fractured and unfractured rocks
  - Some growth strata

- Mahogany oil-shale zone is largely undisturbed

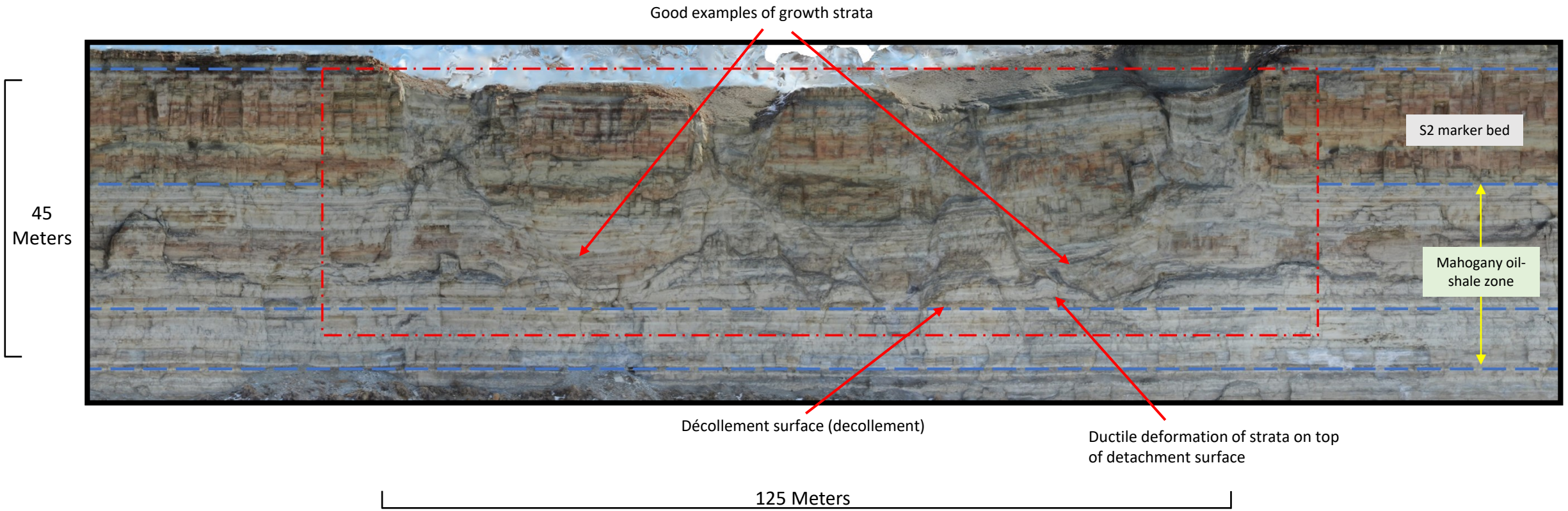

Stratigraphy

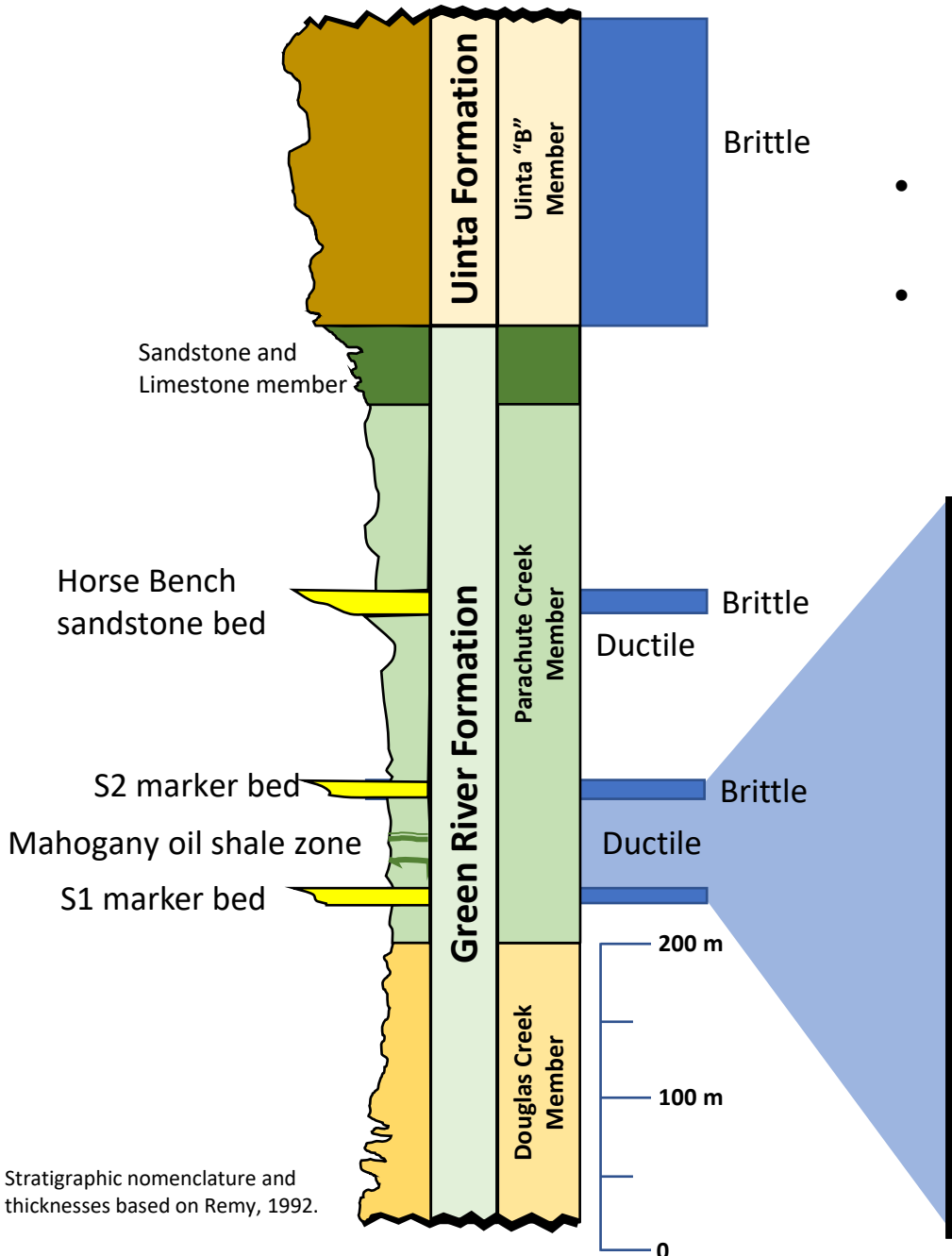

- Brittle sandstones and limestone are broken and sheared in the fault zone
- Ductile oil shales are mostly undeformed
  - Some folding if immediately adjacent to sheared blocks of sandstones

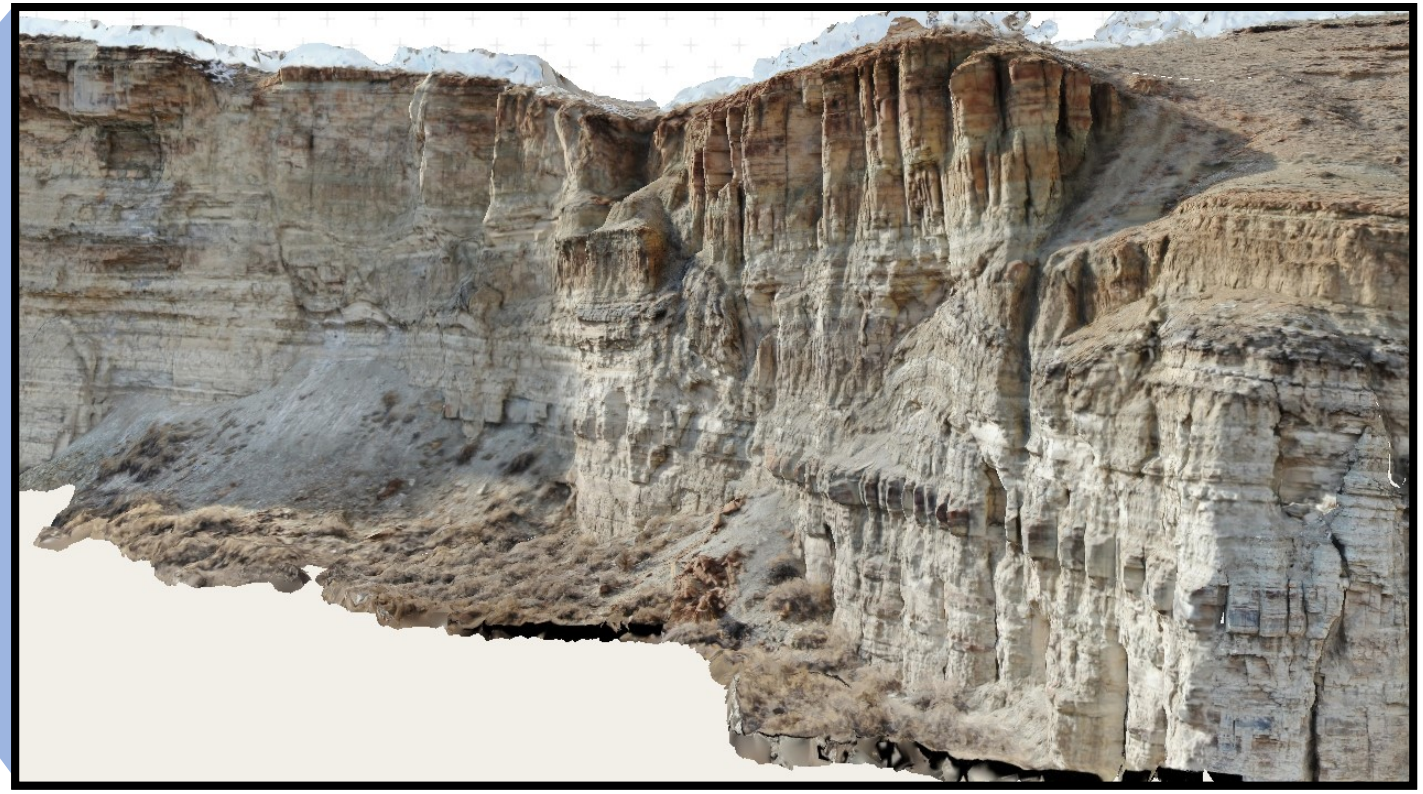

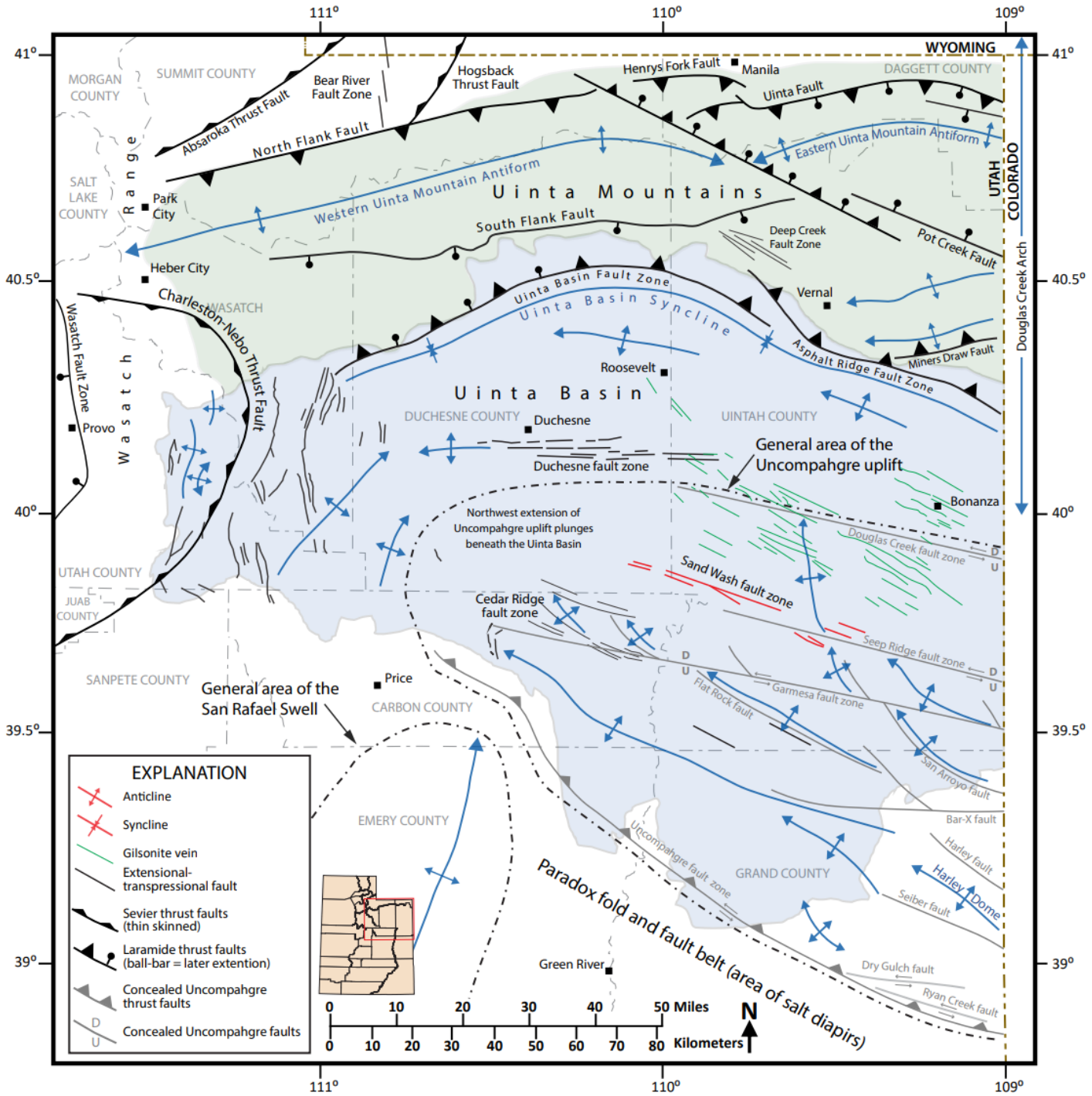

Larger Structural Context

- Tectonic features of the Uinta Basin
- The Sand Wash fault zone is on the outer arc of the Uncompahgre anticline, similar to the Cedar Ridge fault zone
- Deeper structural movement on the SWFZ appears to be linked to deformation on the Uncompahgre Uplift

Modified from Osmond, 1965 and Sprinkel, 2014.

Characterizing the Fault Zone - Fault Trace Lengths

Plan view photo of the SWFZ as an example of methodology of the process of measuring fault length of discreet segments from drone-derived photogrammetry

Fault segment length by stratigraphic unit in meters

Uinta Formation	Sandstone and Limestone Facies	Horse Bench	Parachute Creek Shales and Siltstones	S2
1421	177	406	781	303
429	149	287	685	323
345		375	491	330
434		383	401	317
432		925	252	215
209		642	280	112
158		513	231	157
277		72	408	99
175		31	167	235
543		9	296	259
26		6	150	268
248		250	246	150
308		72	1558	289
140		186	408	155
280		116	1584	111
288		222	520	113
941		38	1096	67
604		111	271	104
363			734	106
197			483	91
477			1039	114
57			135	84
289			150	67
159			393	197
116			208	217
118			90	79
447			81	149
339			235	156
144			119	478
479			1618	522
1481			975	512
791			1079	147
682			758	254
19			336	202
199			99	174
			86	303
			195	435
			98	97
			148	408
			248	80
			129	140
			222	224
			203	66
			380	91
			887	208
			296	331
			475	301
			780	305
			443	297
			332	184
			93	248
			134	184
			169	538
			320	449
			110	296
			106	352
			854	303
			208	237
			63	399
			153	444
			254	295
			588	301
			125	183
			59	103
			74	125
			162	177
			65	107
			206	69
			228	227
			179	64
			25	72
			95	103
			279	18
			127	13
			149	49
			77	91
			138	58
			94	67
			181	48
			78	71
				85
				90
				76
				105
				92
				129
Average Segment Lengths				159
389	163	258	358	196

Characterizing the Fault Zone - Displacements

Segment	Offset (m)		Segment	Offset (m)		Segment	Offset (m)
North Face Nine Mile Mahogany Zone	2.96		South Face Nine Mile S2 Sandstone	1.07		South Face Nine Mile Mahogany Zone	0.278
North Face Nine Mile Mahogany Zone	2.85		South Face Nine Mile S2 Sandstone	1.99		South Face Nine Mile Mahogany Zone	0.879
North Face Nine Mile Mahogany Zone	3.04		South Face Nine Mile S2 Sandstone	1.42		South Face Nine Mile Mahogany Zone	0.713
North Face Nine Mile Mahogany Zone	0.532		South Face Nine Mile S2 Sandstone	1.58		South Face Nine Mile Mahogany Zone	1.12
North Face Nine Mile Mahogany Zone	0.462		South Face Nine Mile S2 Sandstone	1.9		South Face Nine Mile Mahogany Zone	1.58
North Face Nine Mile Mahogany Zone	0.788		South Face Nine Mile S2 Sandstone	1.29		South Face Nine Mile Mahogany Zone	0.782
North Face Nine Mile Mahogany Zone	0.506		South Face Nine Mile S2 Sandstone	0.575		South Face Nine Mile Mahogany Zone	0.762
North Face Nine Mile Mahogany Zone	3.81		South Face Nine Mile S2 Sandstone	1.63		South Face Nine Mile Mahogany Zone	1.42
North Face Nine Mile Mahogany Zone	4.94		South Face Nine Mile S2 Sandstone	0.749		South Face Nine Mile Mahogany Zone	1.28
North Face Nine Mile S2 Sandstone	0.505		South Face Nine Mile S2 Sandstone	4.68		South Face Nine Mile Mahogany Zone	1.21
North Face Nine Mile S2 Sandstone	0.647		South Face Nine Mile S2 Sandstone	2.11		South Face Nine Mile Mahogany Zone	0.39
North Face Nine Mile S2 Sandstone	1.64		South Face Nine Mile S2 Sandstone	2.31		South Face Nine Mile Mahogany Zone	0.232
North Face Nine Mile S2 Sandstone	3.66		South Face Nine Mile S2 Sandstone	2.48		South Face Nine Mile Mahogany Zone	1.23
North Face Nine Mile S2 Sandstone	3.14		South Face Nine Mile S2 Sandstone	1.17		South Face Nine Mile Mahogany Zone	0.606
North Face Nine Mile S2 Sandstone	1.79		South Face Nine Mile S2 Sandstone	1.23		South Face Nine Mile Mahogany Zone	2.04
North Face Reservoir Cliff S2 Sandstor	0.506		South Face Nine Mile S2 Sandstone	1.13		South Face Nine Mile Mahogany Zone	1.63
North Face Reservoir Cliff S2 Sandstor	2.91		South Face Nine Mile S2 Sandstone	2.02		South Face Nine Mile Mahogany Zone	1.21
Ranger Cliff S2 Sandstone	1.24		South Face Nine Mile S2 Sandstone	3.09		South Face Nine Mile Mahogany Zone	2.46
Ranger Cliff S2 Sandstone	1.16		South Face Nine Mile S2 Sandstone	1.02		South Face Nine Mile Mahogany Zone	0.507
Ranger Cliff S2 Sandstone	0.722		South Face Nine Mile S2 Sandstone	0.893		South Face Nine Mile Mahogany Zone	0.266
Ranger Cliff S2 Sandstone	0.774		South Face Nine Mile S2 Sandstone	0.873		South Face Nine Mile Mahogany Zone	0.369
Ranger Cliff S2 Sandstone	0.786		South Face Nine Mile S2 Sandstone	0.602			
Ranger Cliff S2 Sandstone	0.331		South Face Nine Mile S2 Sandstone	0.553			
Ranger Cliff S2 Sandstone	0.351		South Face Nine Mile S2 Sandstone	0.595			
Ranger Cliff S2 Sandstone	0.871		South Face Nine Mile S2 Sandstone	1.05			
Ranger Cliff S2 Sandstone	0.209		South Face Nine Mile S2 Sandstone	1.19			
Ranger Cliff S2 Sandstone	0.159		South Face Nine Mile S2 Sandstone	2.85			
Ranger Cliff S2 Sandstone	0.685		South Face Nine Mile S2 Sandstone	3.14			
Ranger Cliff S2 Sandstone	0.818		South Face Nine Mile S2 Sandstone	0.488			
Ranger Cliff S2 Sandstone	0.195		South Face Nine Mile S2 Sandstone	1.15			
Green River S2 Sandstone	4.49		South Face Nine Mile S2 Sandstone	0.298			
			South Face Nine Mile S2 Sandstone	0.427			
			South Face Nine Mile S2 Sandstone	0.622			
			South Face Nine Mile S2 Sandstone	0.957			
			South Face Nine Mile S2 Sandstone	0.475			
			South Face Nine Mile S2 Sandstone	0.581			
			South Face Nine Mile S2 Sandstone	1.54			
			South Face Nine Mile S2 Sandstone	1.24			
			South Face Nine Mile S2 Sandstone	0.919			
			South Face Nine Mile S2 Sandstone	1.13			
			South Face Nine Mile S2 Sandstone	1.33			

Displacements on discreet fault segments in meters

Methodology of measuring fault displacements

- GPS referenced photographs were taken of the cliff faces
  - Photos were used to build large photogrammetry models
  - Point to point measurements taken to capture throw

- Inclined joints sets (yellow dot) in the rotated fault block in the center of the image
  - Block foundered and rotated after initial jointing

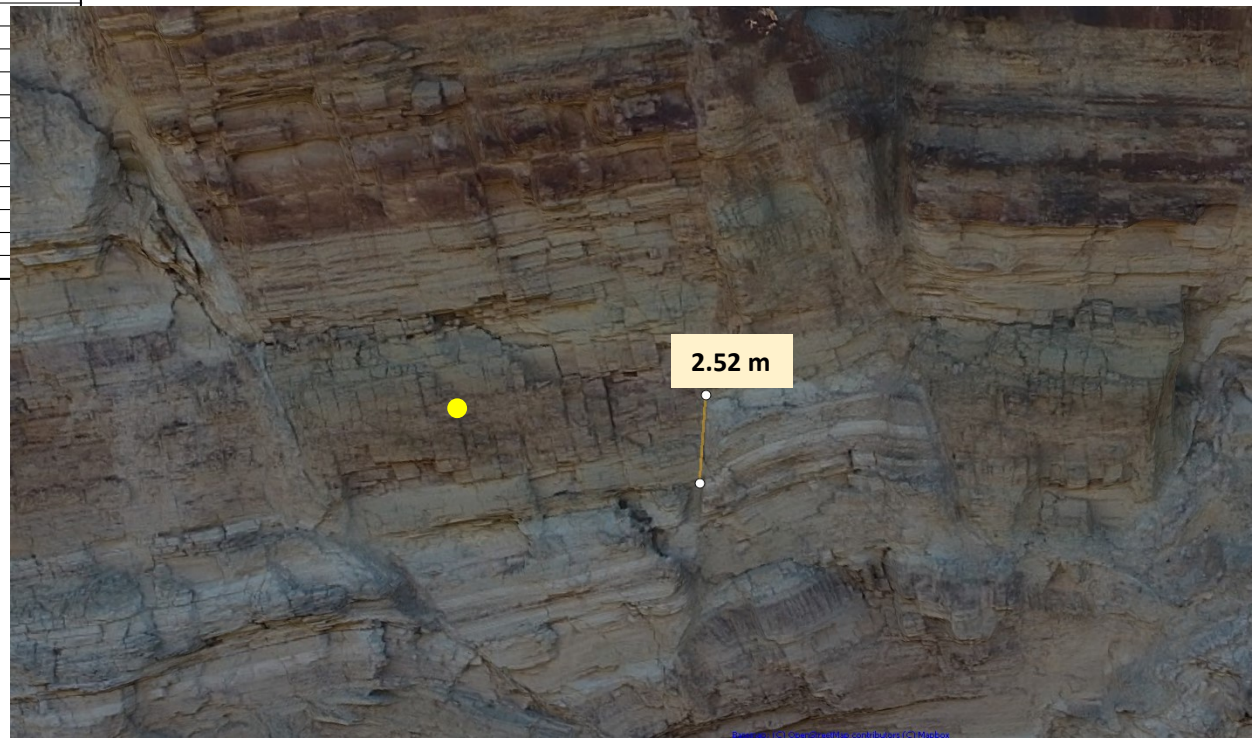

Characterizing the Fault Zone – Fault Planes

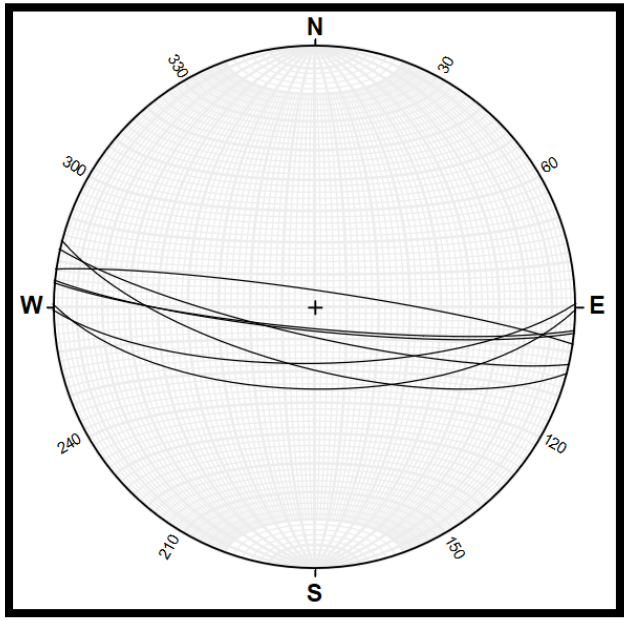

Fault surfaces in the Uinta B Sandstone within a stereograph

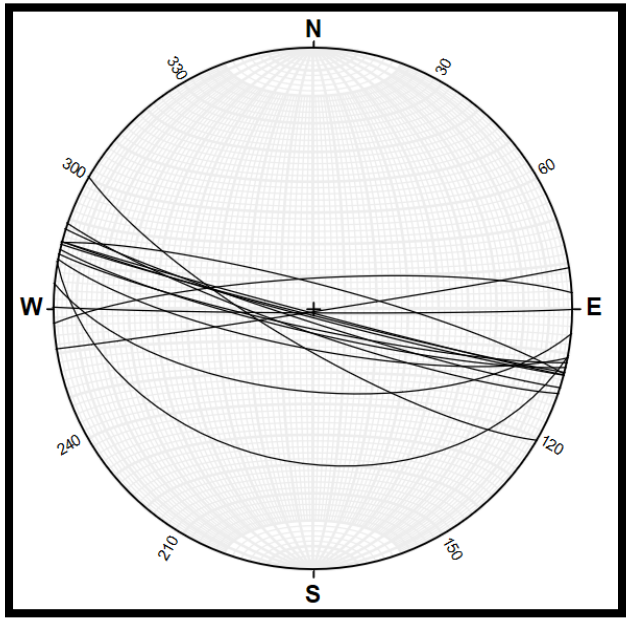

Fault surfaces in the Horse Bench Sandstone

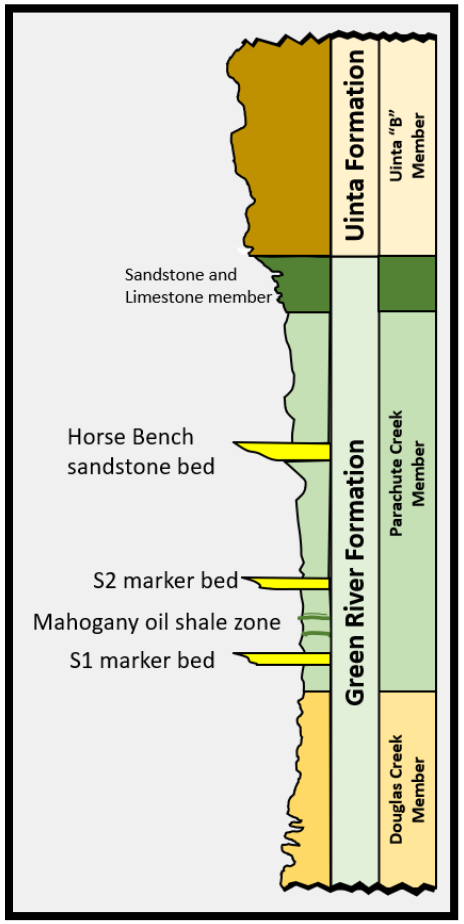

Characterizing the Fault Zone – Fault Planes

No.	Dip	Direction	Latitude	Longitude	Description
1	81.285	13.0994	39.8403045	-109.925779	S2 Sandstone Fault Surface
2	86.87	180.024	39.8403258	-109.925781	S2 Sandstone Fault Surface
3	68.022	357.486	39.8403404	-109.925815	S2 Sandstone Fault Surface
4	75.525	176.659	39.8403894	-109.925805	S2 Sandstone Fault Surface
5	76.09	182.331	39.8404422	-109.925717	S2 Sandstone Fault Surface
6	40.994	183.469	39.8403915	-109.92571	S2 Sandstone Fault Surface
7	84.864	3.47008	39.8404039	-109.925726	S2 Sandstone Fault Surface
8	89.074	9.55065	39.8409621	-109.926934	S2 Sandstone Fault Surface
9	88.572	9.29849	39.8401816	-109.925416	S2 Sandstone Fault Surface
10	83.592	189.304	39.8401801	-109.925425	S2 Sandstone Fault Surface
11	83.119	2.65122	39.8402161	-109.925397	S2 Sandstone Fault Surface
12	65.824	181.611	39.8402324	-109.925413	S2 Sandstone Fault Surface
13	88.299	186.171	39.8404088	-109.924647	S2 Sandstone Fault Surface
14	87.478	8.31604	39.8399985	-109.924339	S2 Sandstone Fault Surface
15	78.931	10.6283	39.8399673	-109.924232	S2 Sandstone Fault Surface
16	70.873	201.065	39.8399463	-109.923335	S2 Sandstone Fault Surface
17	71.024	198.044	39.8398957	-109.922718	S2 Sandstone Fault Surface
18	87.045	198.184	39.8279539	-109.888635	S2 Sandstone Fault Surface
19	82.093	197.35	39.8279643	-109.888605	S2 Sandstone Fault Surface
20	82.219	194.572	39.8280587	-109.888567	S2 Sandstone Fault Surface
21	89.207	196.059	39.8253191	-109.900974	S2 Sandstone Fault Surface
22	76.606	22.6407	39.8399985	-109.924339	S2 Sandstone Fault Surface
23	85.782	184.642	39.8399673	-109.924232	S2 Sandstone Fault Surface
24	68.81	1.49503	39.8399463	-109.923335	S2 Sandstone Fault Surface
25	76.841	188.139	39.8398957	-109.922718	S2 Sandstone Fault Surface
26	77.431	186.123	39.8403915	-109.92571	S2 Sandstone Fault Surface
27	77.354	192.162	39.8404039	-109.925726	S2 Sandstone Fault Surface
28	83.765	188.335	39.8409621	-109.926934	S2 Sandstone Fault Surface
29	43.218	181.775	39.8401816	-109.925416	S2 Sandstone Fault Surface
30	84.986	2.46196	39.8401801	-109.925425	S2 Sandstone Fault Surface
31	77.971	8.85322	39.8402161	-109.925397	S2 Sandstone Fault Surface
32	81.191	17.2268	39.8401801	-109.925425	S2 Sandstone Fault Surface
33	66.003	26.0501	39.8402161	-109.925397	S2 Sandstone Fault Surface
34	71.12	227.519	39.8402324	-109.925413	S2 Sandstone Fault Surface
35	65.407	170.765	39.8404088	-109.924647	S2 Sandstone Fault Surface
36	71.9	184.363	39.8399985	-109.924339	S2 Sandstone Fault Surface
37	84.865	176.323	39.8399673	-109.924232	S2 Sandstone Fault Surface
38	86.555	195.934	39.8399463	-109.923335	S2 Sandstone Fault Surface
39	73.094	205.523	39.8403045	-109.925779	S2 Sandstone Fault Surface
40	67.708	213.78	39.8403258	-109.925781	S2 Sandstone Fault Surface
41	71.635	203.688	39.8403404	-109.925815	S2 Sandstone Fault Surface
42	87.267	19.7466	39.8403894	-109.925805	S2 Sandstone Fault Surface

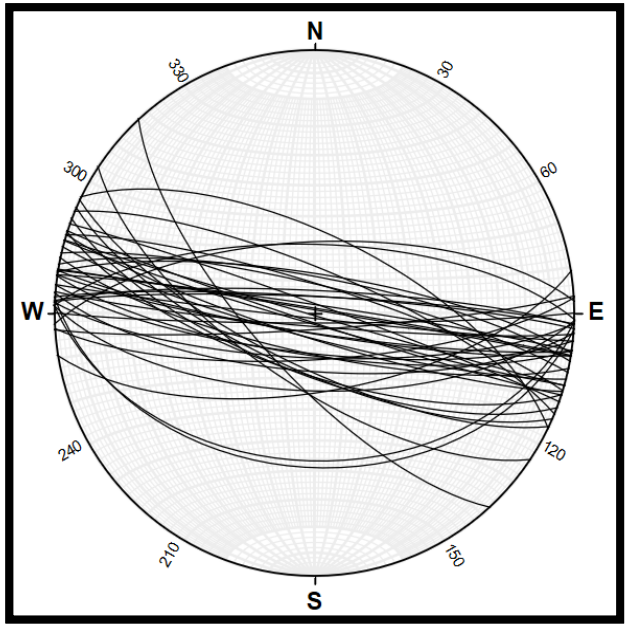

Fault surfaces in the S2 marker bed

Fault surface dips, dip directions and locations for the S2 marker bed

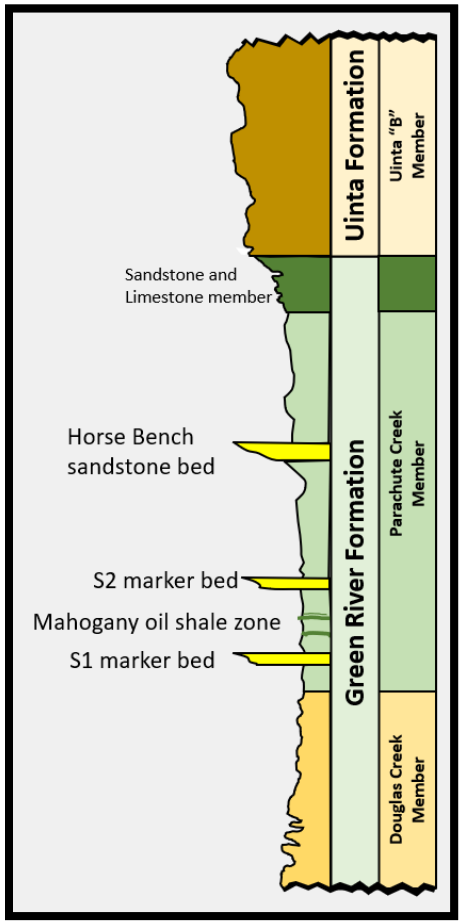

Characterizing the Fault Zone – Syndepositional Fault Movement

- Well-developed decollement surface under a series of fault blocks that were also deformed
  - Likely because they were newly deposited and poorly lithified while being deformed
- Syndepositional healed surfaces and growth strata also indicate syndepositional movement on this fault

- Large, rotated blocks with fault drag and shortening on the footwall
  - Indicating poor lithification and deformation early after burial

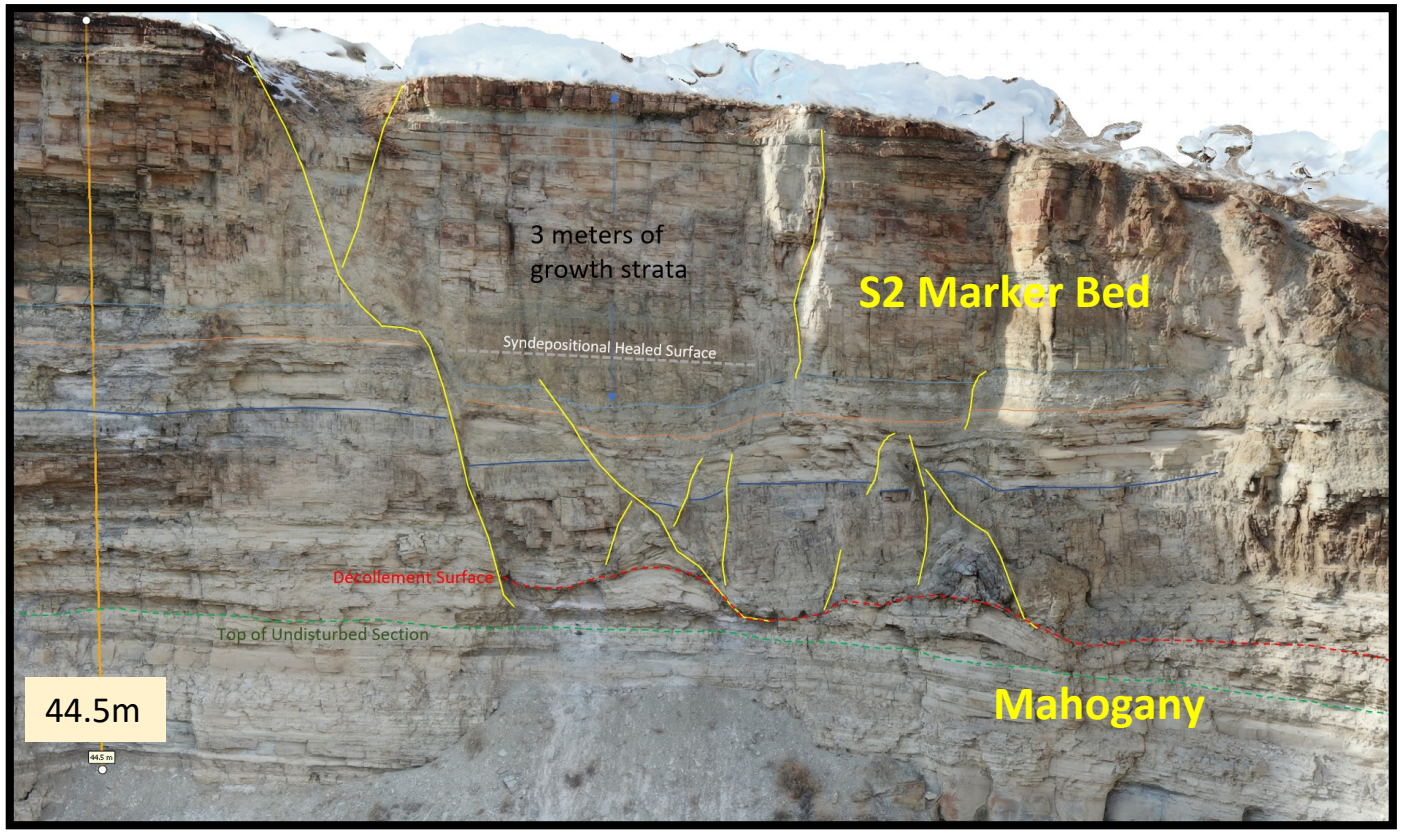

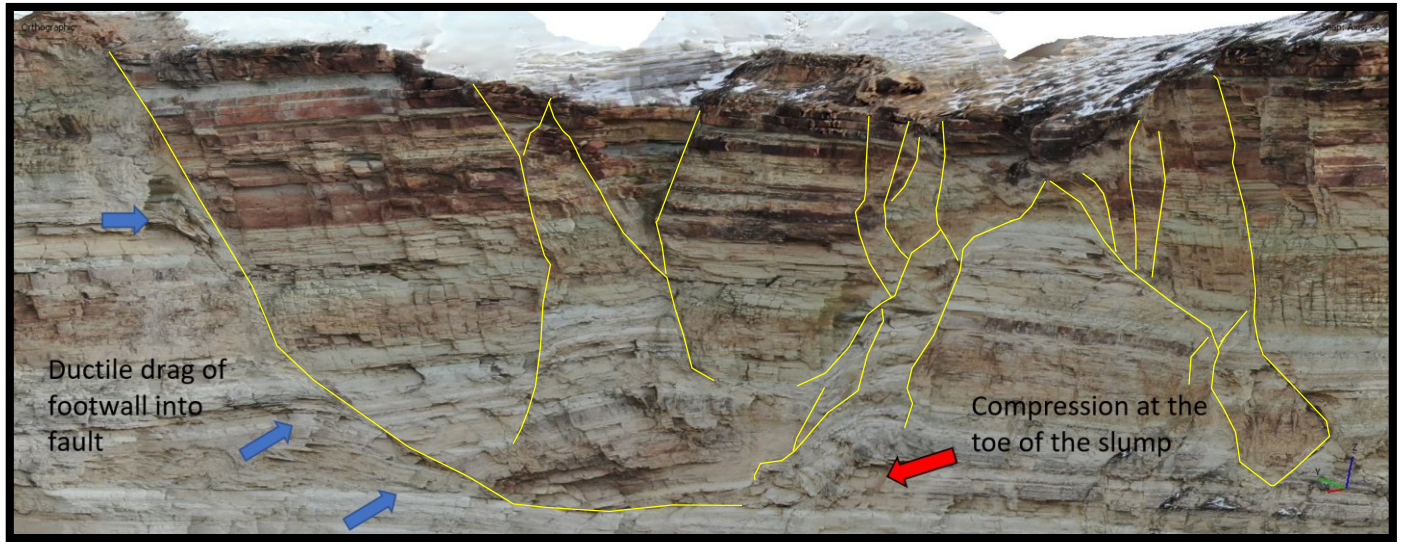

Characterizing the Fault Zone – Slickenlines

No.	Plunge	Trend	Latitude	Longitude	Description
1	76.3888	202.952	39.8605	-110.009	Uinta Formation Slickenlines
2	60.567	204.556	39.8604	-110.009	Uinta Formation Slickenlines

Fault surface slickenlines plunges, trends, and locations for the Uinta Formation

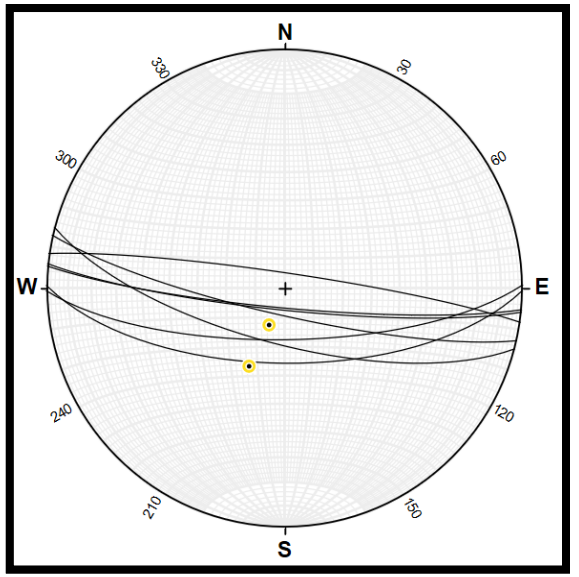

Stereograph of slickenlines posted on fault surfaces from the Uinta Formation, member B.

Fault surface slickenlines plunges, trends and locations for the Horse Bench Sandstone

No.	Plunge	Trend	Latitude	Longitude	Description
1	83.0785	92.3898	39.8429	-109.938	Horse Bench Sandstone Slickenlines
2	74.5114	160.314	39.8429	-109.938	Horse Bench Sandstone Slickenlines
3	37.365	193.586	39.8428	-109.938	Horse Bench Sandstone Slickenlines
4	83.3084	203.815	39.8436	-109.933	Horse Bench Sandstone Slickenlines

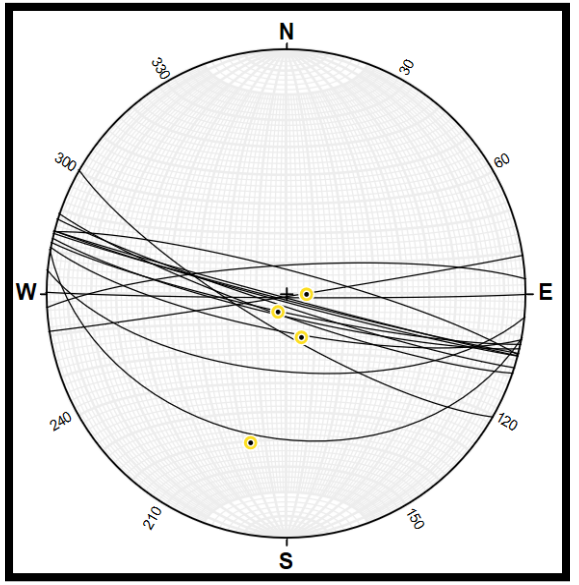

Slickenlines posted on fault surfaces from the Horse Bench Sandstone.

Characterizing the Fault Zone – Slickenlines

Stereograph of slickenlines posted on fault surfaces from the S2 marker bed

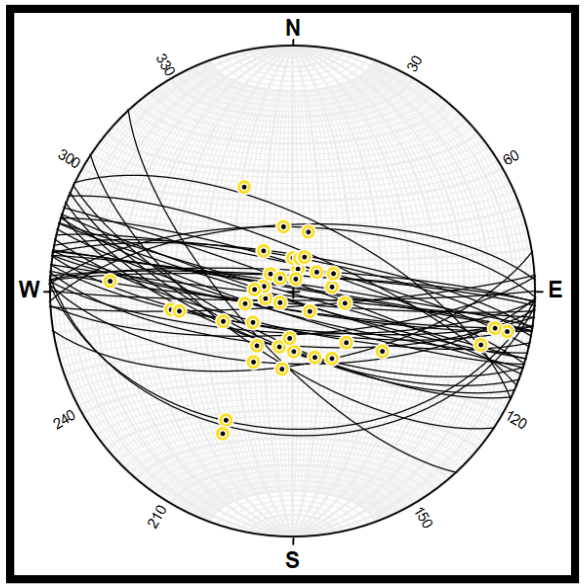

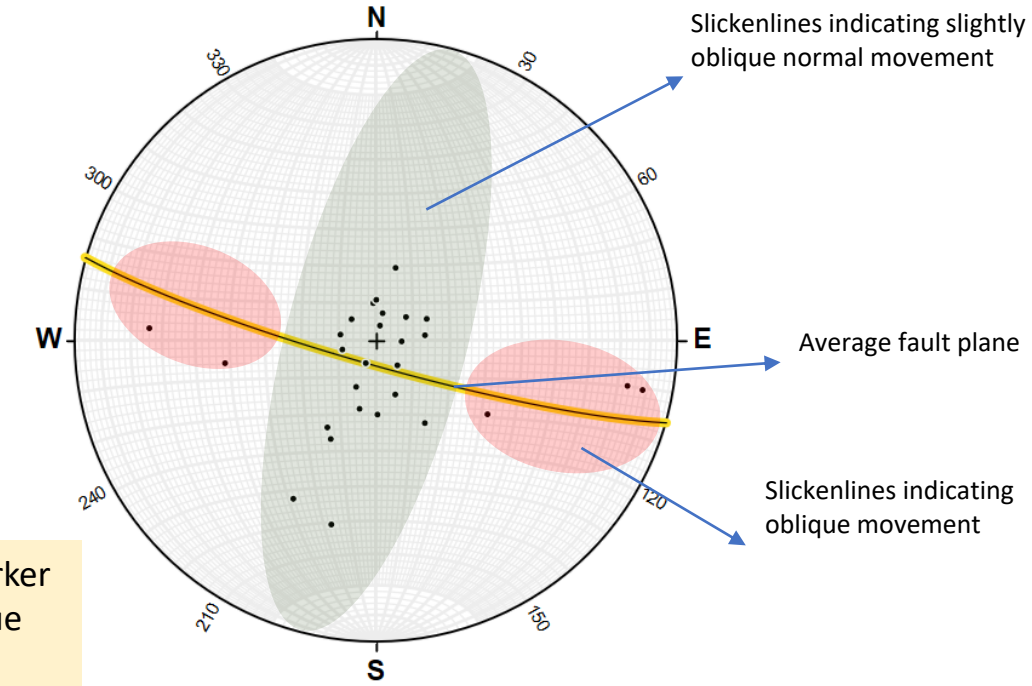

Slickenlines from the S2 marker bed, with dip slip and oblique slip slickenlines

Sense of Movement

- Near vertical fault surface contains at least three generations of slickenlines, demonstrating changes on the fault over time
- Slickenlines marked in red are the oldest as subsequent slickenlines overprint them
    - These mostly strike-slip slickenlines were created when the fault was moving in a sinistral oblique direction
- Later the fault moved in an oblique dextral direction
    - Then again in a more normal dextral sense of motion
- These changing slip directions can be seen in the stereograph
    - The fault surface is represented as a great circle
    - The slickenlines are represented as points
    - The points are numbered in chronological order of slip (1 is oldest)

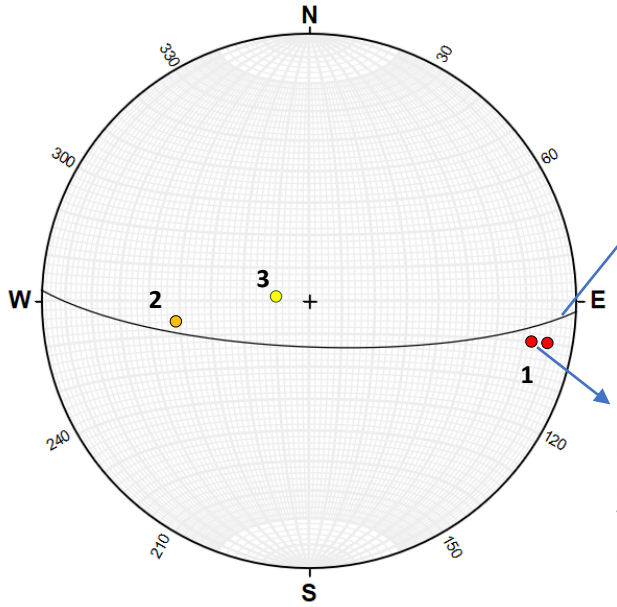

Uninterpreted

Interpreted

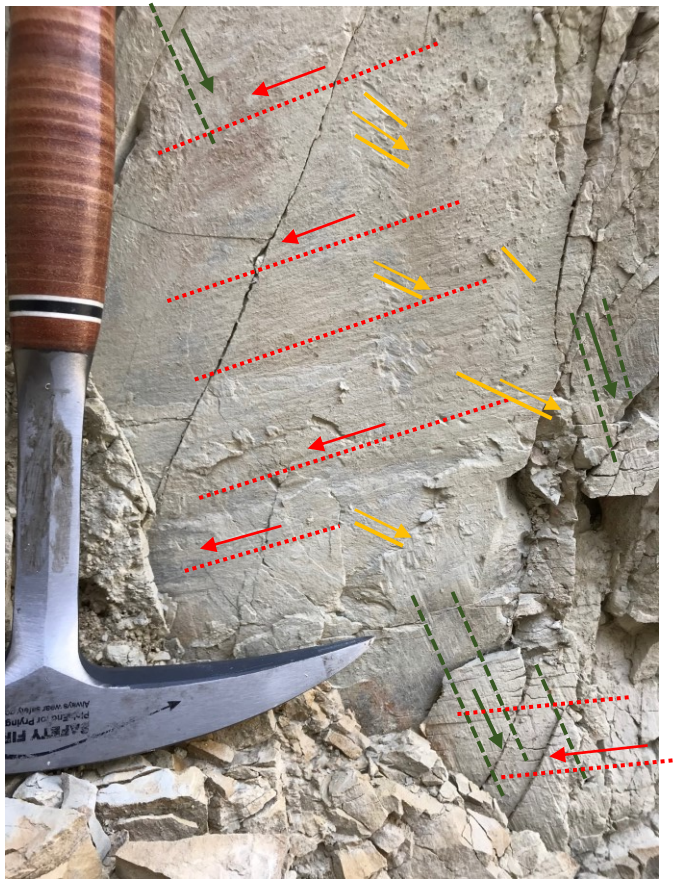

Explanation

First set of slickensides with sinistral oblique transpressional slip

Second set of slickensides with oblique dextral normal slip

Third set of slickensides with oblique dextral normal slip

Characterizing the Fault Zone – Fractures

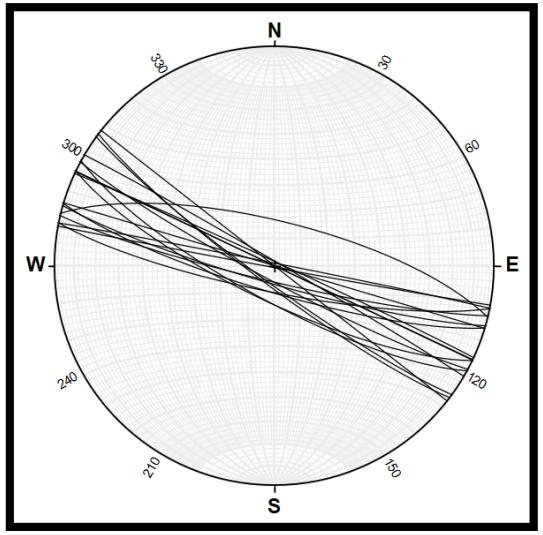

Stereograph of joint sets within the Sand Wash fault zone

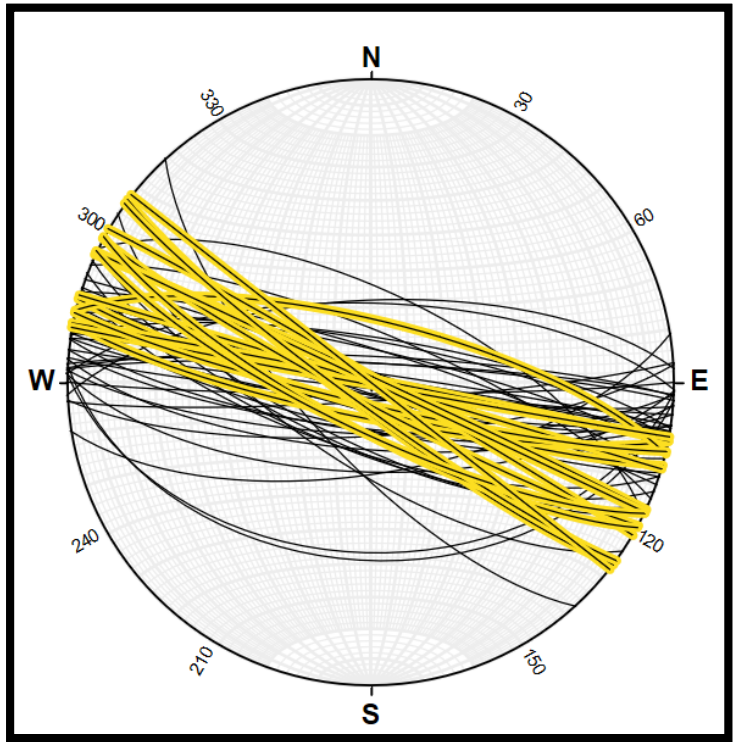

Stereograph of joint sets (yellow) compared to fault surfaces (black)

-There is a 5° clockwise rotation of average of the joint sets

Extensive jointing in the Horse Bench sandstone within the SWFZ

Jointing is denser at the top of the Horse Bench in the cleanest sandstones and decreases in density downward

Characterizing the Fault Zone – Folds

We collected fold axial-plane dip and dip direction data defining the axial surface of folds in the Mahogany bed and the lower S2 marker bed

Stereograph of axial surfaces for each fold

The surface in yellow is the average of all the Mahogany folds, roughly paralleling fault and joint azimuths

These parallel the fault zone and represent deformation related to the grabens

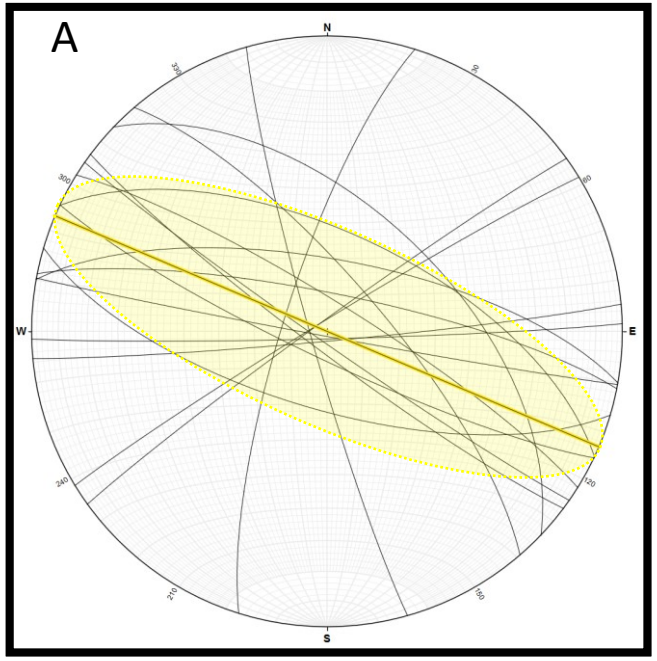

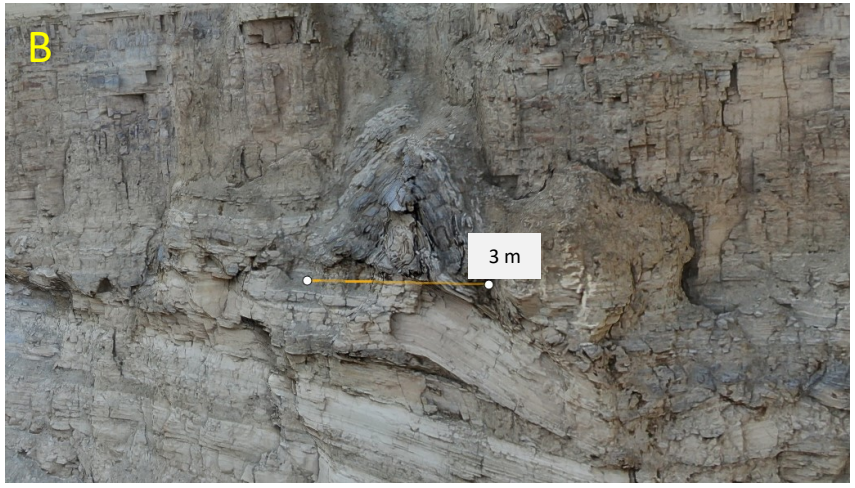

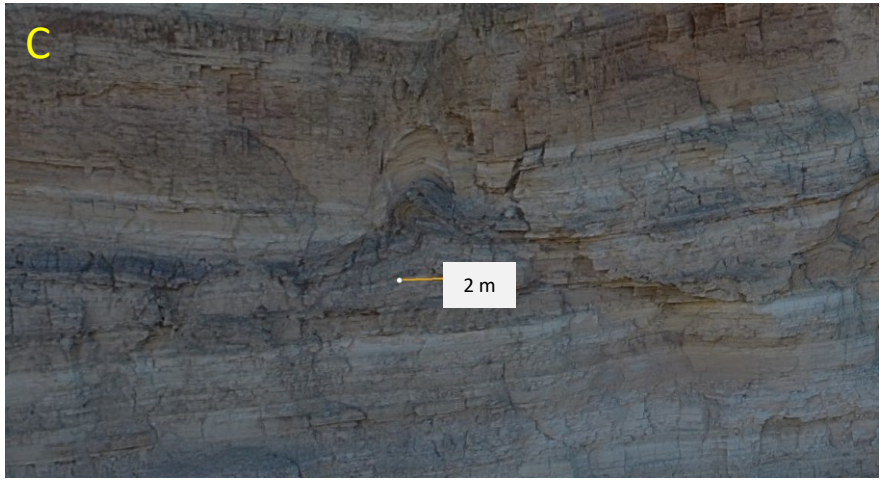

Characterizing the Fault Zone – Dikes

- Dikes are useful to identify the local stress fields from when they were intruded
- These dikes are in a specific stratigraphic interval across the study area
  - Interpreted to be emplaced contemporaneously to deformation on the fault zone
- Within the SWFZ, maximum horizontal stress was NW-SE
  - Parallel to the fault zone
- On the margins of the SWFZ, maximum horizontal stress was NE-SW
  - Perpendicular to the fault zone

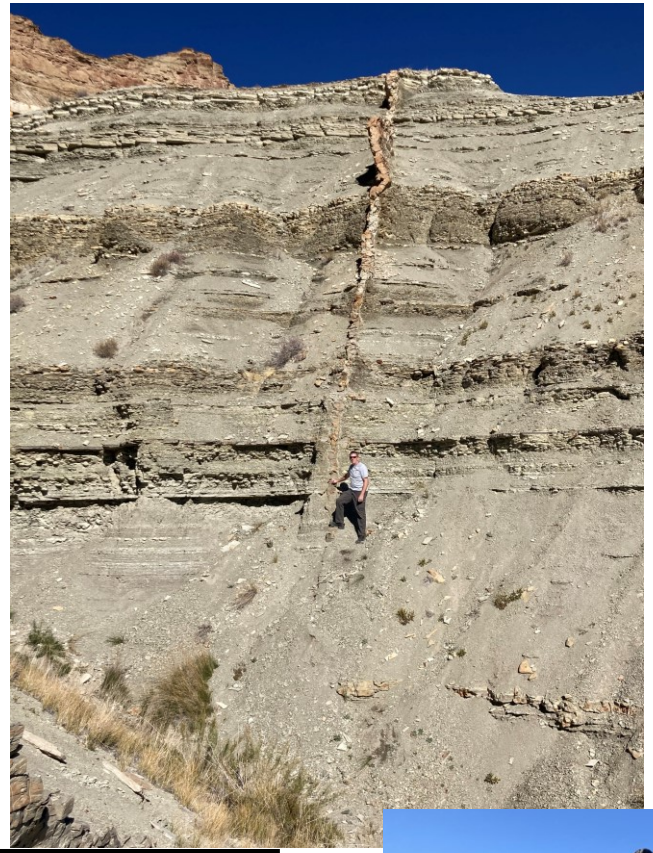

Dikes within the SWFZ are parallel to the trend of faults

Dikes on the margin of the SWFZ are perpendicular to the trend of faults

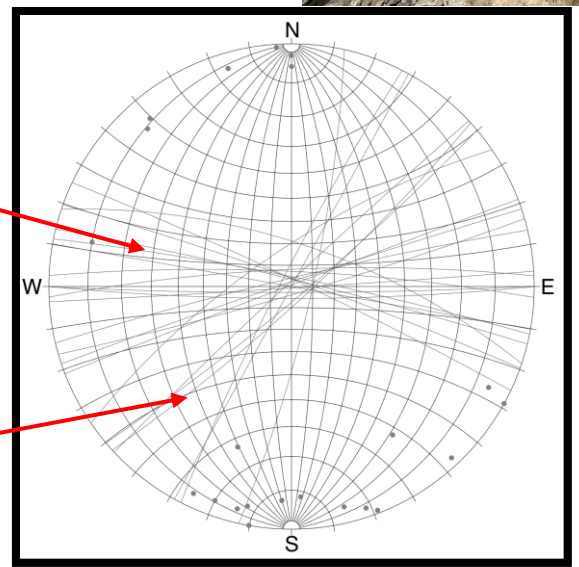

Characterizing the Fault Zone – Breccia Dikes

- Breccia dike (outlined in red) that intruded a fault in the Uinta Formation in the SWFZ

- The fault contains slickenlines demonstrating dip slip
  - The 2-meter-wide dike does not exhibit brittle deformational features
  - The fault has likely not moved since intrusion

- This breccia dike parallels and has similarities to the famous gilsonite veins 10 kilometers to the north
  - The dike likely intruded contemporaneously with the gilsonite veins in Oligocene during initial extension in the Uinta Basin

Characterizing the Fault Zone – Decollement Surfaces

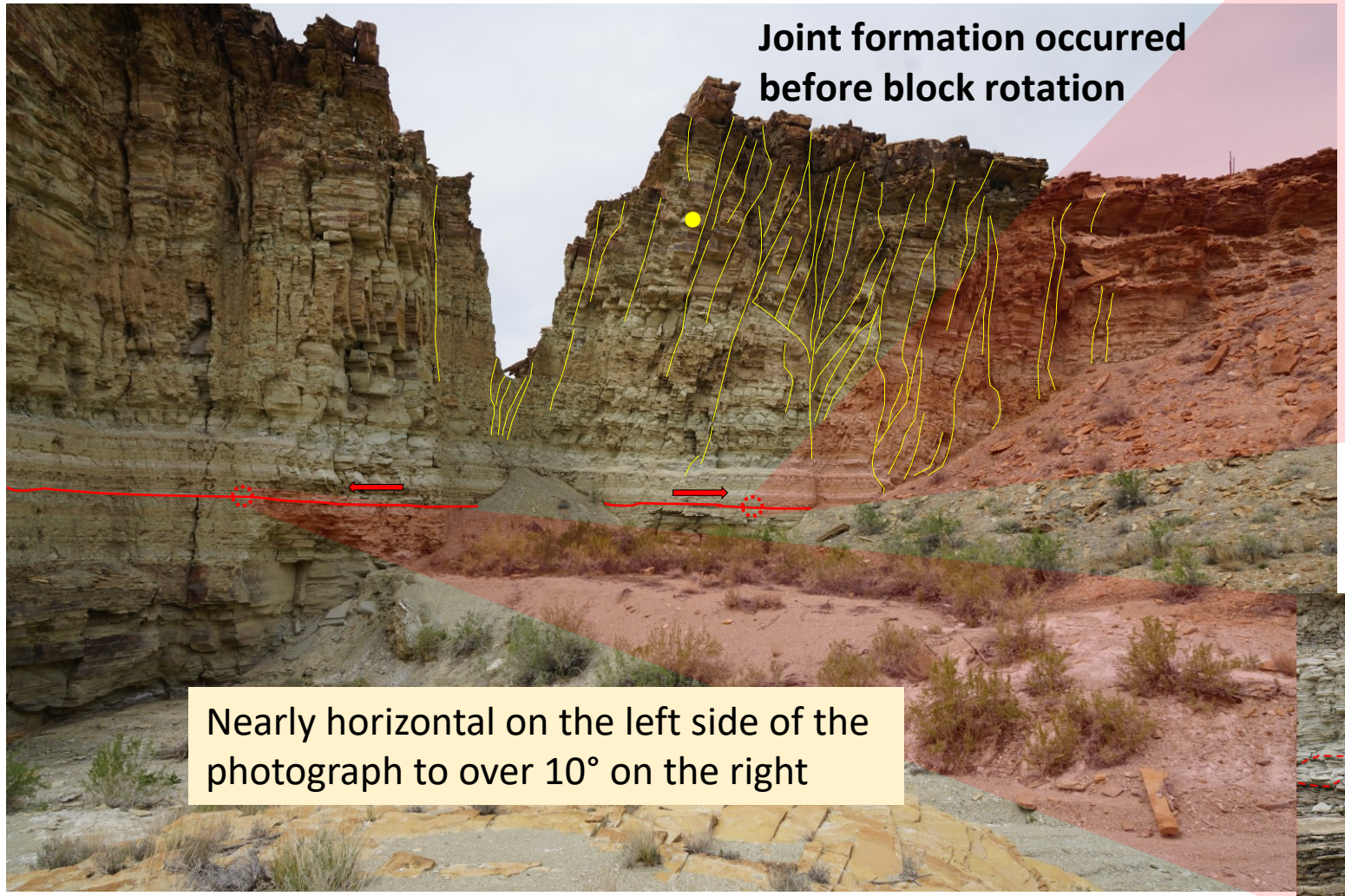

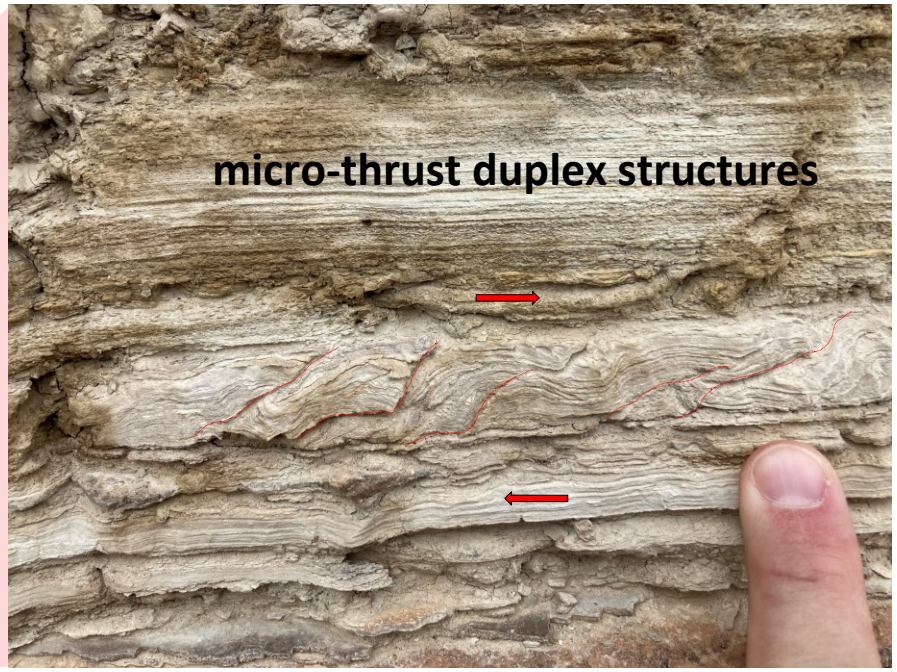

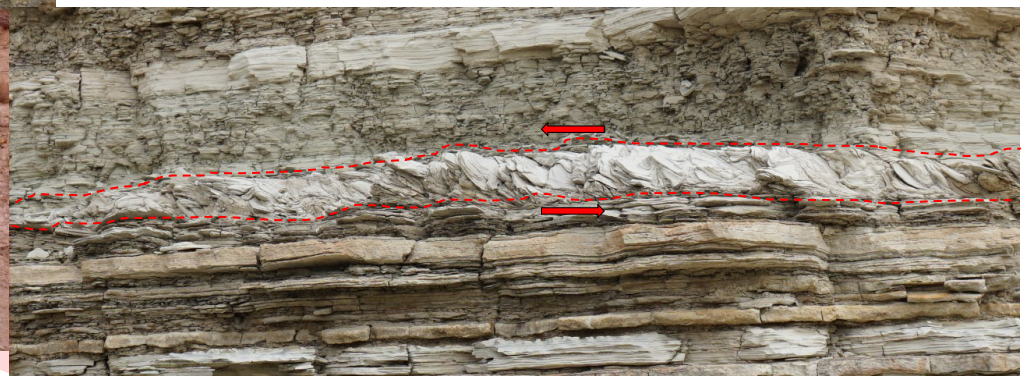

Characterizing the Fault Zone – Small Sag Basins

- Small sag basin near the top of the Mahogany zone
  - The sag basin is filled with a heterolithic mixture of mudstones and siltstones
  - Capped by an undeformed “healed surface”

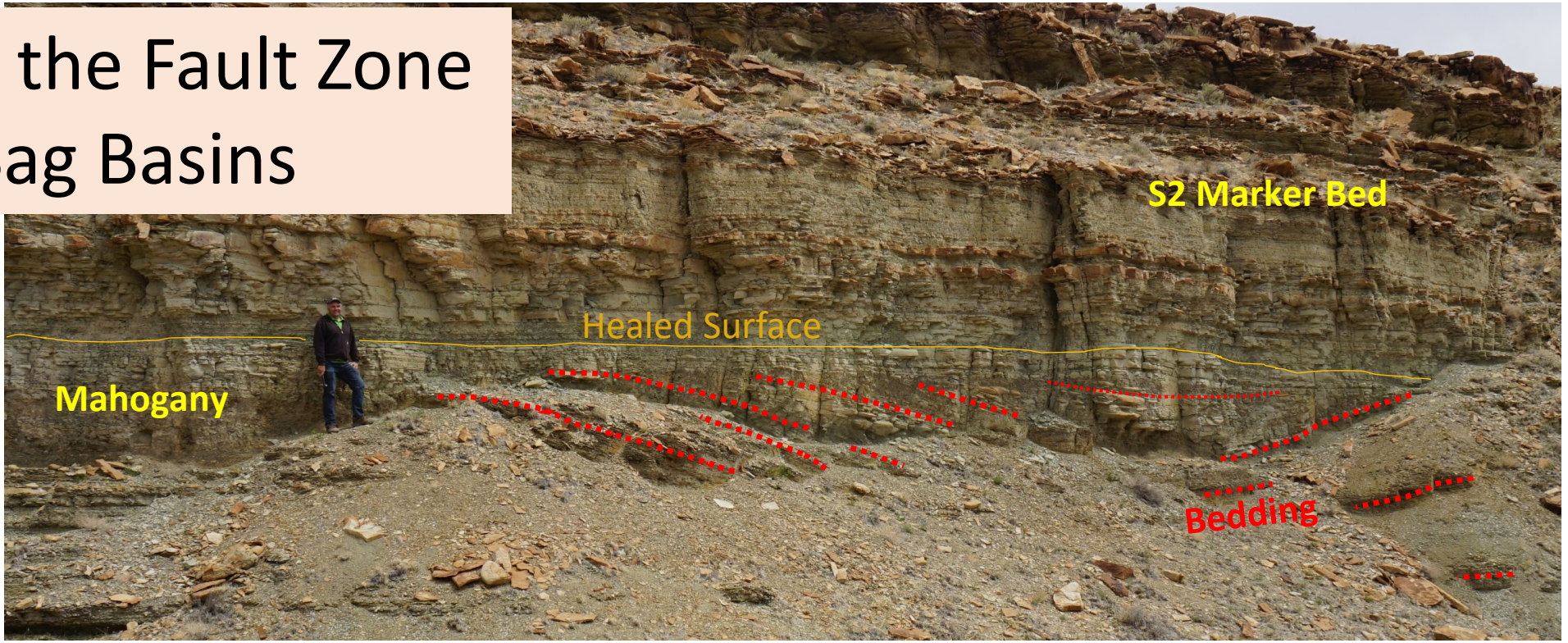

- Larger sag basin found on a cliff face of the Mahogany zone near the Green River
- It also is filled with a heterolithic mixture but is much larger in scale.

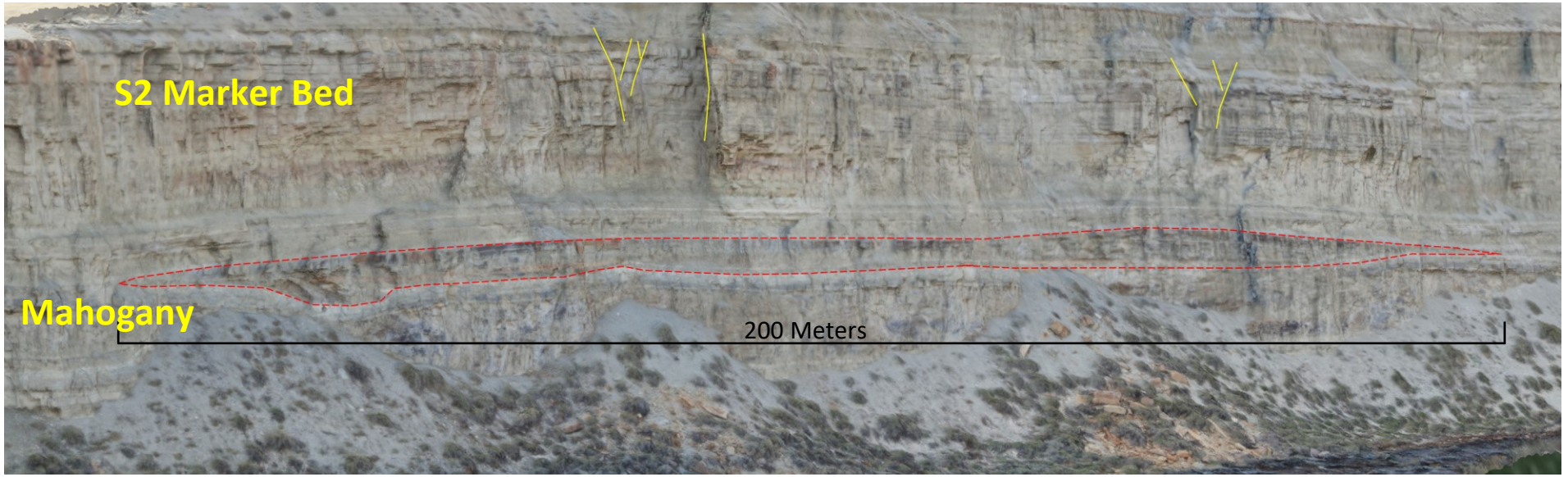

Characterizing the Fault Zone – Bed Orientations

- Stratigraphic dips, dip directions, and locations were measured across the SWFZ
- The steepest dips are within the fault zone on rotated blocks
- Dips on the north flank of the fault zone are steeper than to the south

3° increase in dip across the SWFZ on the S2 Marker SS

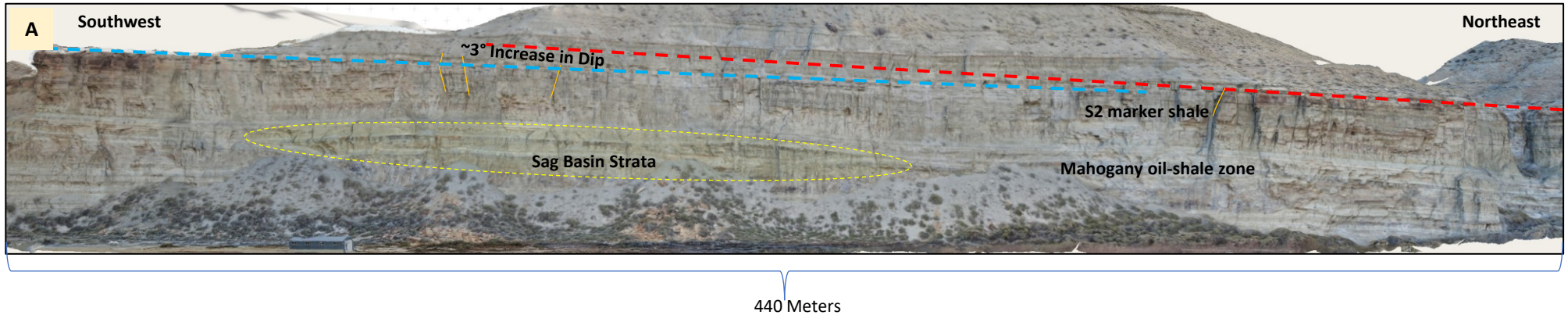

440 Meters

3° increase in dip across the SWFZ on the S2 Marker SS

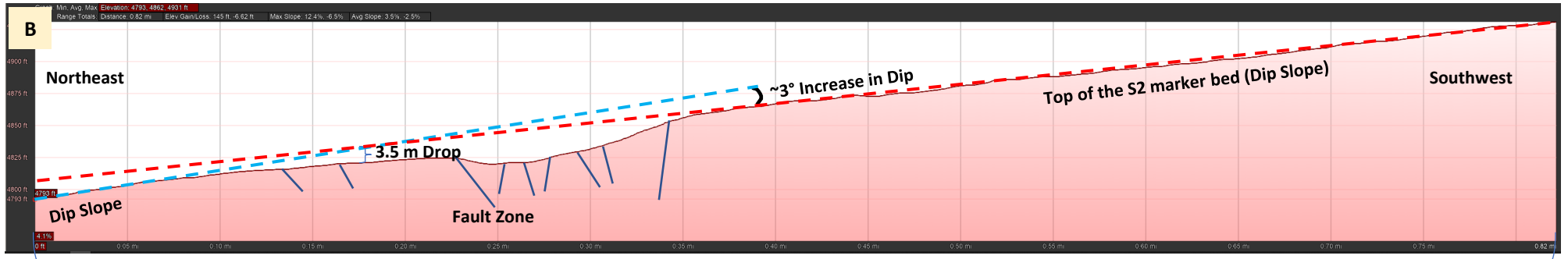

1320 Meters

3° increase in dip across the SWFZ on the Horse Bench SS

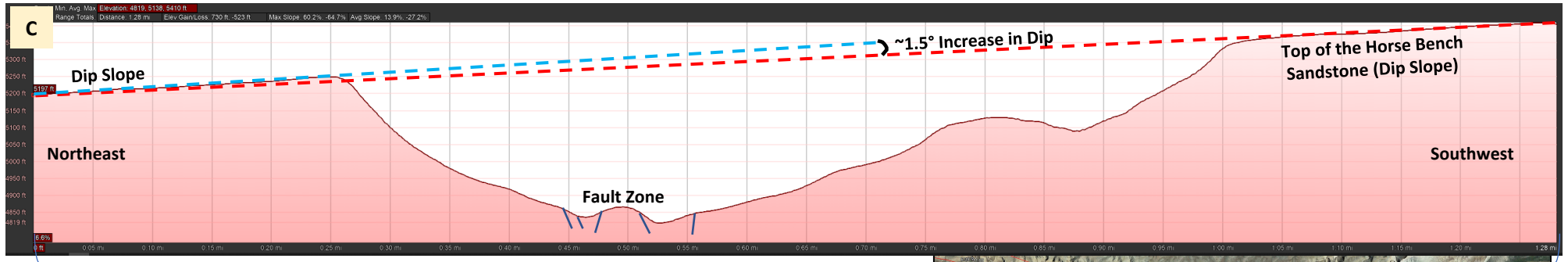

2060 Meters

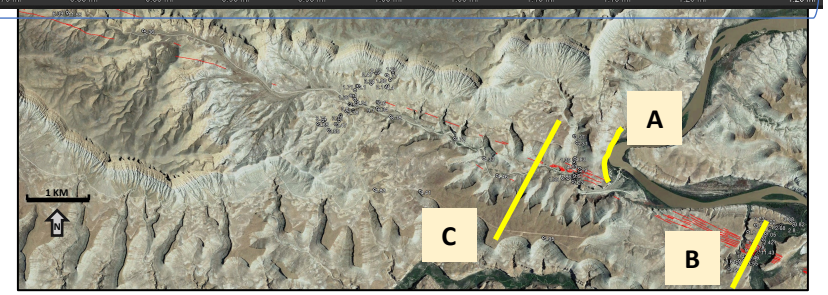

Proximate Cause of the Faulting

SWFZ Deformation Model: Extension Above the Neutral Surface of a Large Fold

- Our model is that extension above the neutral surface of a large fold is being accommodated by the SWFZ
  - Fits observed faults geometries, sag basins and dikes
- The fold is the result of faulting on much deeper rocks
- Nearby seismic images deep faulting on adjacent structures

Faults, grabens, sag basins and parallel dikes

Perpendicular dikes on the margin of the fold

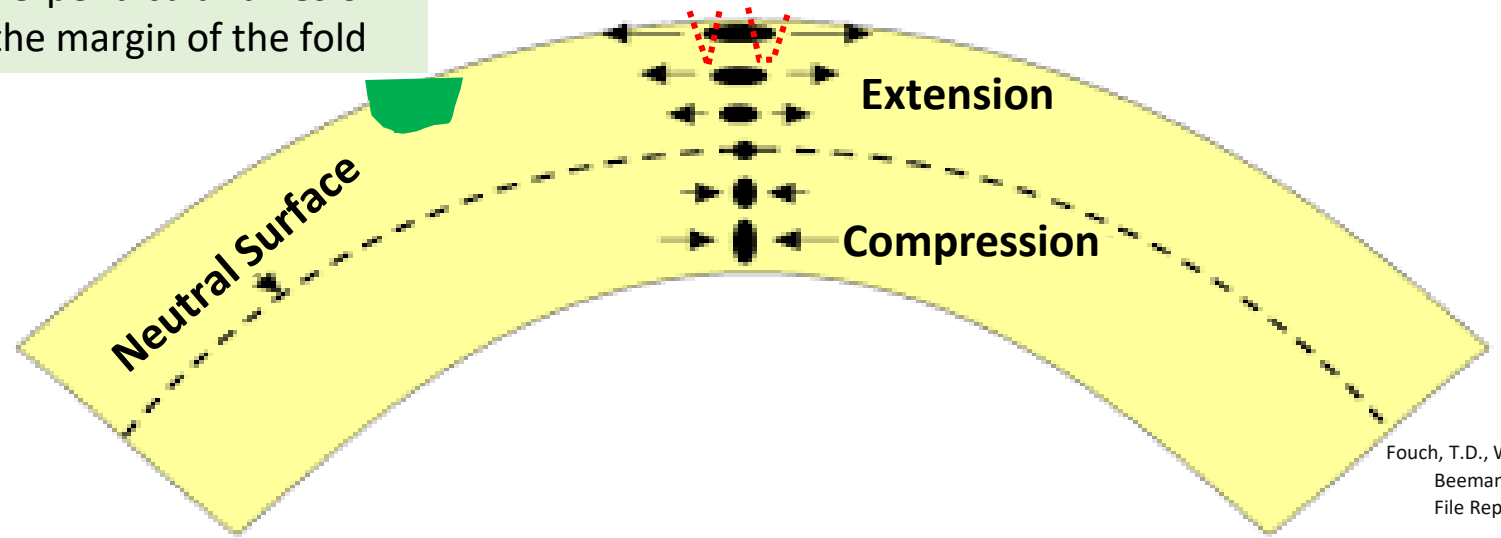

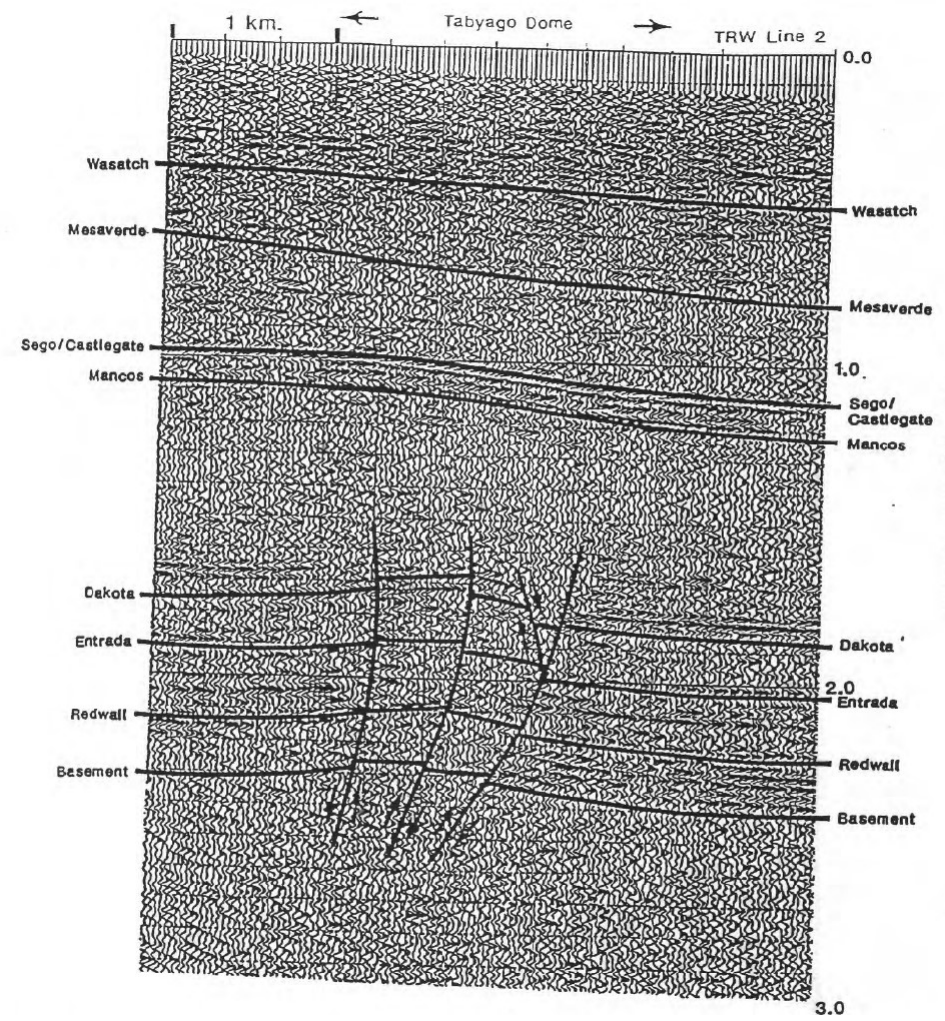

Fouch, T.D., Wandrey, C.J., Taylor, D.J., Butler, C.B., Miller, J.J., Prensky, S.E., Boone, L.E., Schmoker, J.W., Crovelli, R.A., Beeman, 1994b, Oil and Gas Resources of U.S. Naval Oil Shale Reserves 1 and 3, Colorado, and Reserve 2, Utah: Open-File Report 94-427, U.S. Department of Energy Contract No. DE-AT21-93-MC30141, https://doi.org/10.3133/ofr94427.

SWFZ Matches Mapped Basement Faults

- Area basement faults and antiforms are related to the Uncompahgre uplift
- Many of these faults are features that are only partially expressed in the overlying sedimentary cover
- Note the consistent trend of the structures and their relationship with the SWFZ

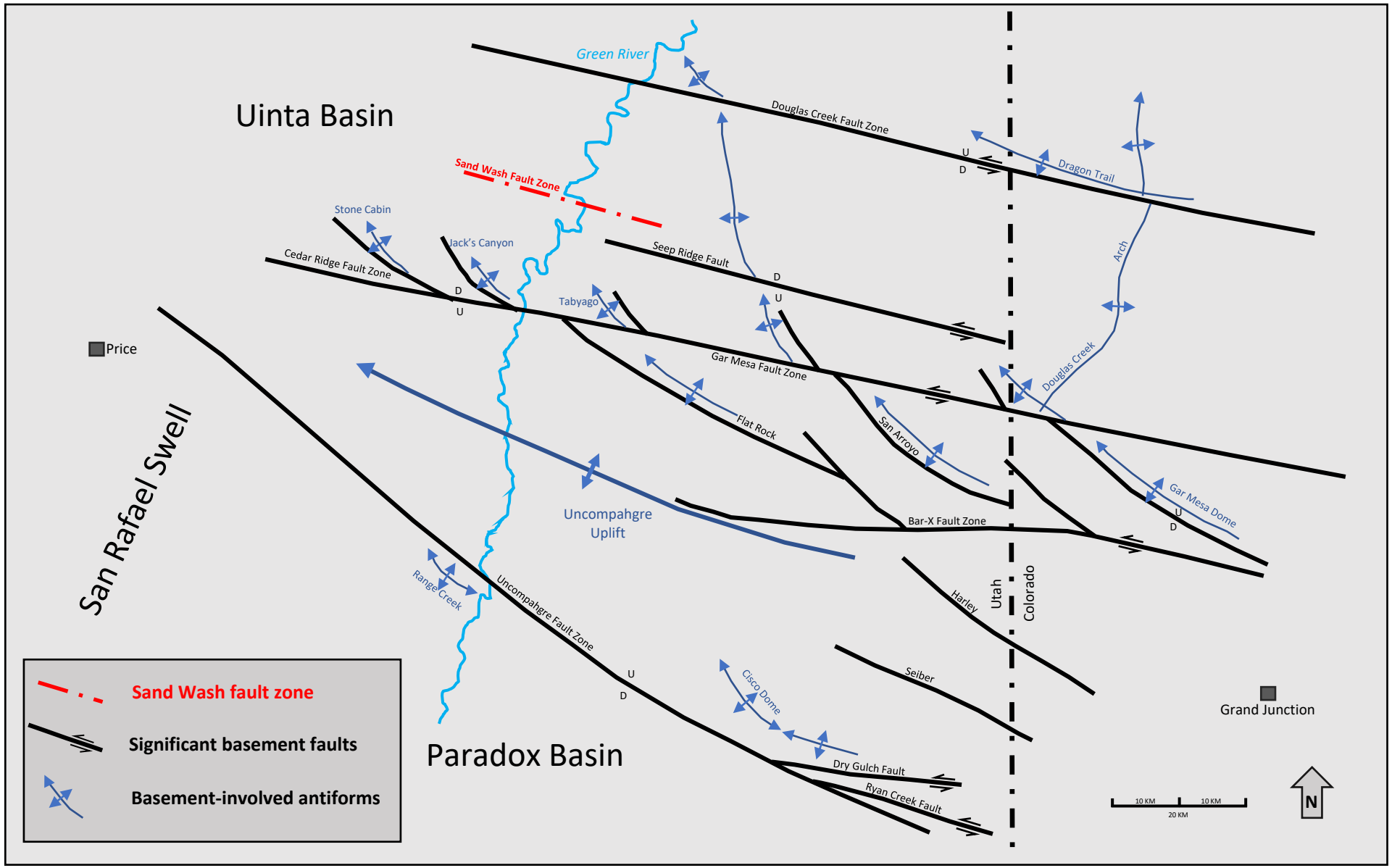

Modified from Stone (1977), and Eckels and others (2004).

Why are the Sandstones So Heavily Fault and the Oil Shales Not?

- Simple rock mechanics
- The sandstones are much more brittle at any given TOC than the shales

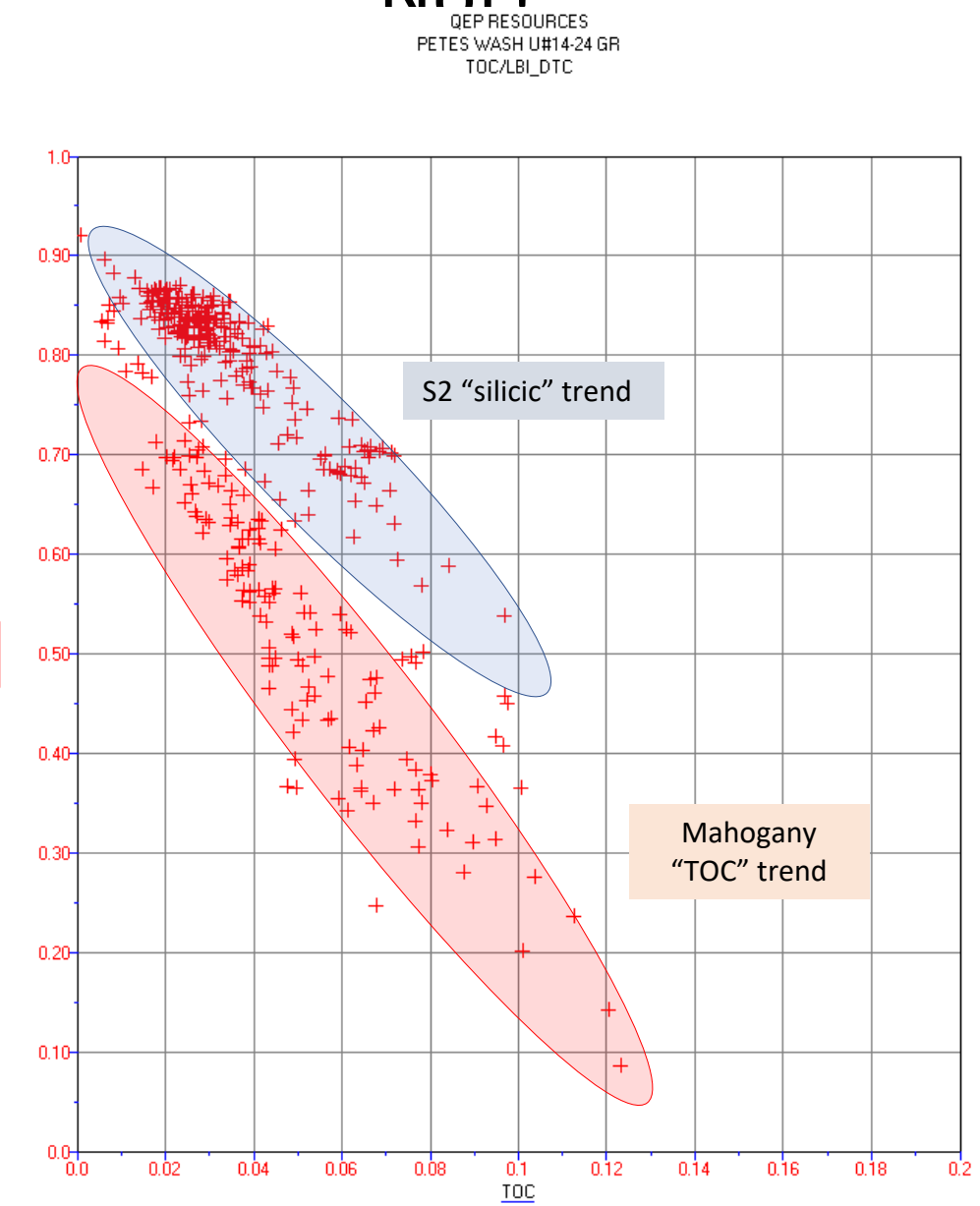

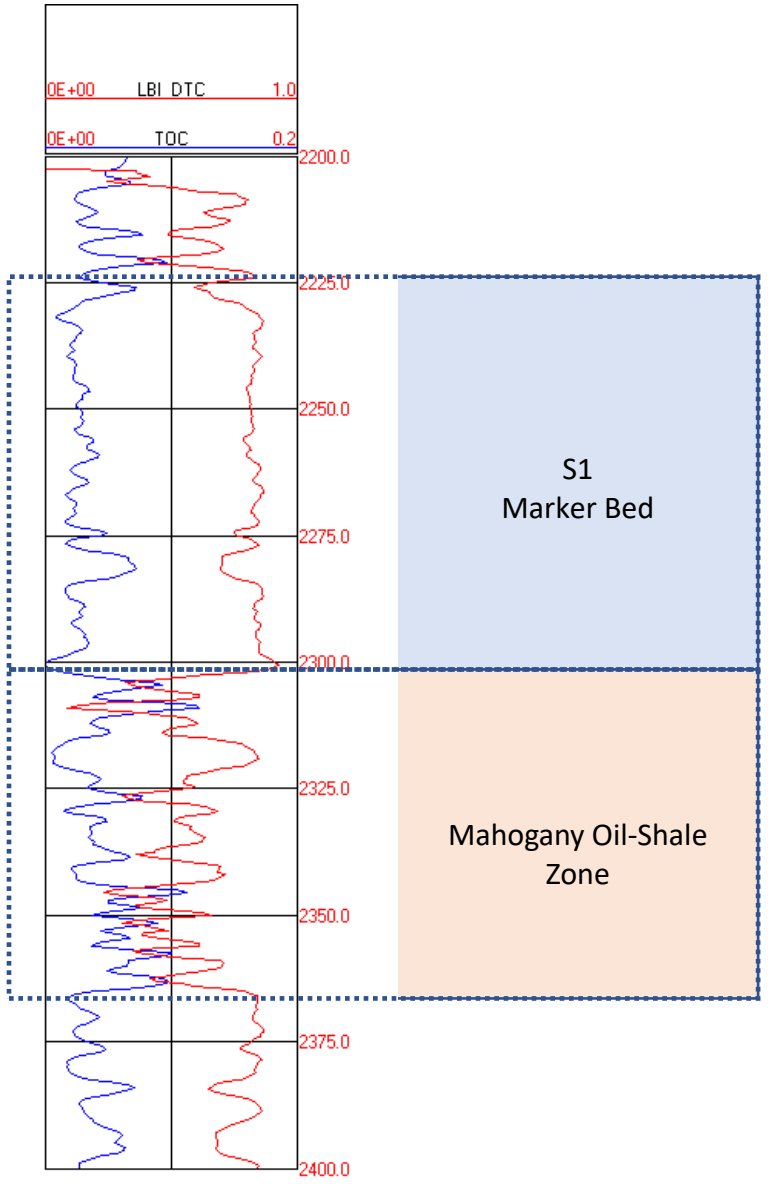

Deformation Model

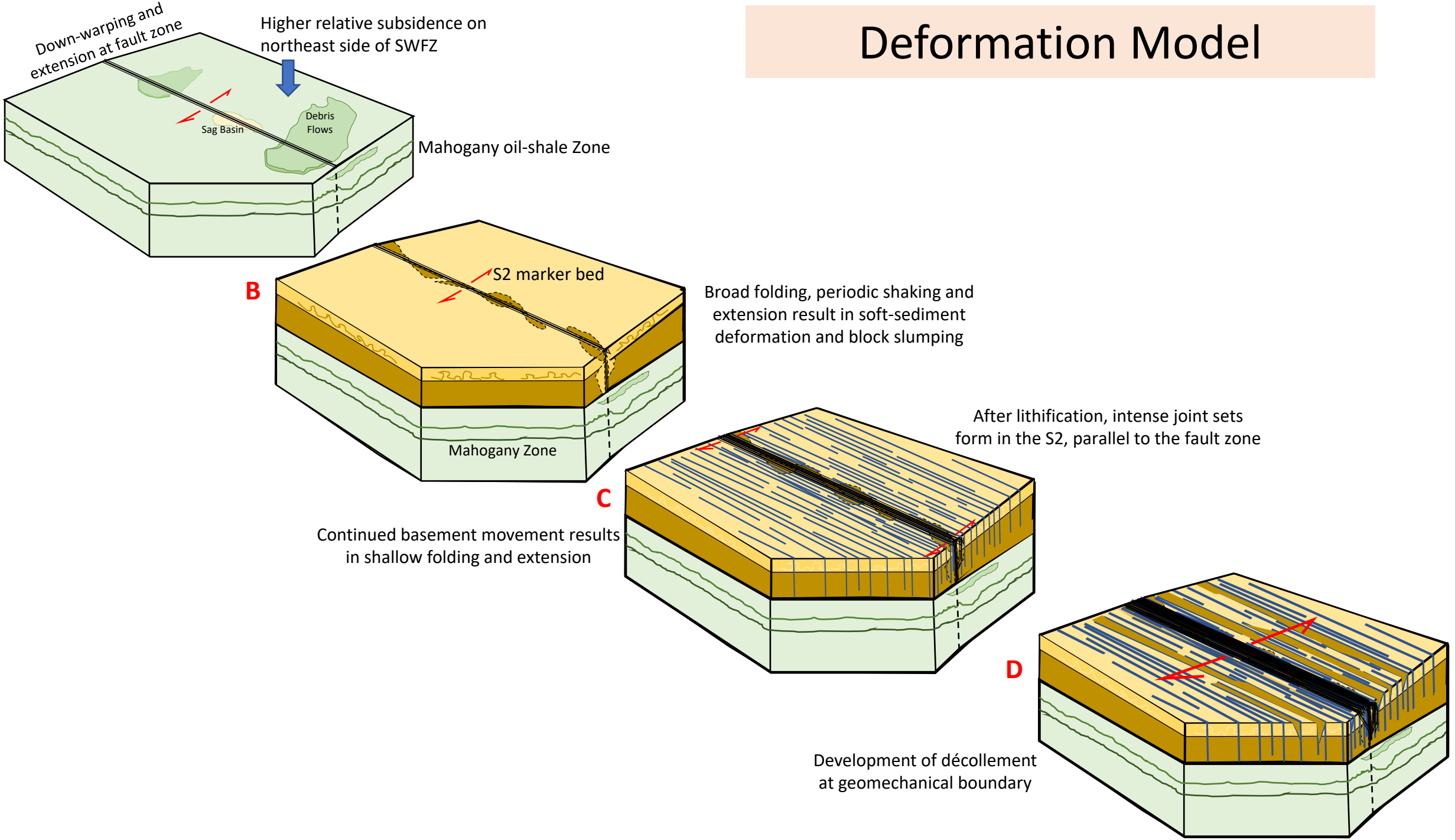

References

- Aslan, A., Karlstrom, K.E., Kirby, E., Heizler, M.T., Granger, D.E., Feathers, J.K., Hanson, P.R., and Mahan, S.A., 2019, Resolving time-space histories of Late Cenozoic bedrock incision along the Upper Colorado River, USA: Geomorphology, v. 347, p. 1–26, doi: https://doi.org/10.1016/j.geomorph.2019.106855.
- Bader, J.W., 2008, Structural and tectonic evolution of the Cherokee Ridge arch, south-central Wyoming—implications for recurring strike-slip along the Cheyenne belt suture zone: Rocky Mountain Geology, v. 43, no. 1, p. 23–40.
- Bader, J.W., 2009, Structural and tectonic evolution of the Douglas Creek arch, the Douglas Creek fault zone, and environs, northwestern Colorado, and northeastern Utah—implications for petroleum accumulation in the Piceance and Uinta Basins:
- Rocky Mountain Geology, v. 44, no. 2, p.121–145. Birgenheier, L.P., and Vanden Berg, M.D., 2011, Core-based integrated sedimentologic, stratigraphic, and geochemical analysis of the oil shale bearing Green River Formation, Uinta Basin, Utah: U.S. Department of Energy, National Energy Technology Laboratory, Topical Report, 19 p. Boden, T., and Tripp, B.T., 2012, Gilsonite veins of the Uinta Basin, Utah: Utah Geological Survey Special Study 141, 48 p., ISBN 978-155791-856-7.
- Bradley, W.H., 1931, Origin and microfossils of the oil shale of the Green River Formation of Colorado and Utah: U.S. Geological Survey Professional Paper 168, 58 p.
- Brinkerhoff, R., 2019, Characterizing outcrop growth faults, slump blocks, mud volcanoes and other sedimentary deformation features for use as reservoir analogues for observed features in targeted reservoirs in the Green River Formation, Uinta Basin, Utah [abs.]: American Association of Petroleum Geologists, Rocky Mountain Section Meeting, Search and Discovery Article #51623.
- Brinkerhoff, R., and Millard, M., 2019, Using pore system characterization to subdivide the burgeoning Uteland Butte play, Green River Formation, Uinta Basin, Utah [abs.]: American Association of Petroleum Geologists, Rocky Mountain Section Meeting, Search and Discovery Article #11272.
- Brinkerhoff, R., and Sprinkel, D.A., 2021, Uinta enigma—the Duchesne fault zone and its impact on the development of the Uinta Basin: Rocky Mountain Association of Geologists, The Outcrop, v. 70, no. 3, p. 16–30.
- Cashion, W.B., 1967, Geology and fuel resources of the Green River Formation, southeastern Uinta Basin, Utah and Colorado: U.S. Geological Survey Professional Paper 548, 48 p.
- Davis, S.J., Mix, H.T., Weigand, B.A., Carroll, A.R., and Chamberlain, C.P, 2010, Synorogenic evolution of large-scale drainage patterns—isotope paleohydrology of sequential Laramide basins: American Journal of Science, v. 309, p. 549–602.
- Dickinson, W.R., Lawton, T.F., and Inman, K.F., 1986, Sandstone detrital modes, central Utah foreland region—stratigraphic record of Cretaceous-Paleogene tectonic evolution: Journal of Sedimentary Petrology, v. 56, no. 2, p. 276–293.
- Eckels, M.T., Suek, D.H., Harrison, D.H., and Harrison, P.J., 2004, North Hill Creek 3-D seismic exploration project: Ute Indian Tribe, Uintah & Ouray Reservation, Uintah County: U.S Department of Energy, Final Technical Report, 26 p.
- Ford, G.L., Pyles, D.R., and Dechesne, M., 2016, Stratigraphic architecture of a fluvial-lacustrine basin-fill succession at Desolation Canyon, Uinta Basin, Utah—reference to Walthers' Law and implications for the petroleum industry: The Mountain Geologist, v. 53, no. 1, p. 5–28.
- Fouch, T.D., 1976, Revision of the lower part of the Tertiary system in the central and western Uinta Basin, Utah: U.S. Geological Survey Bulletin 1405-C, p. C1–C7.
- Fouch, T.D., Cashion, W.B., Ryder, R.T., and Campbell, J.A., 1976, Field guide to lacustrine and related nonmarine depositional environments in Tertiary rocks, Uinta Basin, Utah, in Epis, R.C., and Weimer, R.J., editors, Professional contributions of Colorado School of Mines-studies in Colorado field geology, Number 8: Colorado School of Mines, p. 358–385.
- Fouch, T.D., Nuccio, V.F., Anders, D.E., Rice, D.D., Pitman, J.K., and Mast, R.F., 1994a, Green River (!) petroleum system, Uinta Basin, Utah, U.S.A., *in* Magoon, L.B., and Dow, W.G., editors, The petroleum system—from source to trap: American Association of Petroleum Geologists Memoir 60, p. 399–421.
- Fouch, T.D., Wandrey, C.J., Taylor, D.J., Butler, C.B., Miller, J.J., Prensky, S.E., Boone, L.E., Schmoker, J.W., Crovelli, R.A., Beeman, 1994b, Oil and Gas Resources of U.S. Naval Oil Shale Reserves 1 and 3, Colorado, and Reserve 2, Utah: Open-File Report 94-427, U.S. Department of Energy Contract No. DE-AT21-93-MC30141, https://doi.org/10.3133/ofr94427.
- Grabowski, G.J., Jr., and Peaver, D.R., 1985, Sedimentology and petrology of profundal lacustrine sediments, Mahogany zone of the Green River Formation, Piceance Creek Basin, northwest Colorado, *in* Crevello, P.D., and Harris, P.M., editors, Deep-water carbonates—buildups, turbidites, debris flows and chalk: Society for Sedimentary Geology (SEPM) Core Workshop 6, p. 386–430. Grout, M.A., and Verbeek, E.R., 1998, Tectonic and paleostress significance of the regional joint network of the central Paradox Basin, Utah and Colorado: U.S. Geological Survey Bulletin 2158, p.151–166.
- Howe, J., and Klinger, R., 2021, Evidence for Quaternary activity on the Duchesne-Pleasant Valley fault, Uinta Basin, Utah: Seismological Society of America Seismological Research Letters, v. 92, no. 2B, p. 1335, doi: https://doi.org/10.1785-/0220210025.

References

- Johnson, R.C., 1985, Early Cenozoic history of the Uinta and Piceance Creek Basins, Utah and Colorado, with special reference to the development of Eocene Lake Uinta, *in* Flores R.M., and Kaplan, S.S., editors, Cenozoic paleogeography of the west-central United States: Society for Sedimentary Geology (SEPM), Rocky Mountain Section, Rocky Mountain Paleogeography Symposium 3, p. 247–276, online, http://archives.datapages.com/data/rocky_sepm/data/023/023001/247_rocky_mount230247.htm.
- Johnson, R.C., and Finn, T.M., 1986, Cretaceous through Holocene history of the Douglas Creek arch, Colorado and Utah, *in* Stone, D.S., editor, New interpretations of northwest Colorado geology: Rocky Mountain Association of Geologists Guidebook, p. 77–95.
- Karlstrom, K.E., Crow, R., Crossey, L.J., Coblentz, D., and Van Wijk, J.W., 2008, Model for tectonically driven incision of the younger than 6 Ma Grand Canyon: Geology, v. 36, no. 11, p. 835, doi: 10.1130/g25032a.1.
- Keighley, D., 2013, Outcrop chemostratigraphic correlation of the upper Green River Formation in the Uinta Basin, Utah—Mahogany oil shale zone to the Uinta Formation: Utah Geological Survey Miscellaneous Publication 13-1, p. 30.
- Keighley, D., Töro, B., Vanden Berg, M.D., and Pratt, B.R., 2015, Deformation within the Mahogany oil shale zone of the Green River Formation at Sand Wash, eastern Utah, USA, *in* Vanden Berg, M.D., Ressetar, R., and Birgenheier, L.P., editors, Geology of Utah's Uinta Basin and Uinta Mountains: Utah Geological Association Publication 44, p. 423–438.
- Marshak, S., Nelson, W.J., and McBride, J.H., 2003, Phanerzoic strike-slip faulting in the continental interior platform of the United States: examples from the Laramide Orogen, Midcontinent, and Ancestral Rocky Mountains, *from*: Storti, F., Holdsworth, R.E. and Salvani, F. (eds) *Intraplate Strike-Slip Deformation Belts.* Geological Society, London, Special Publications, 210, 159-184, 0305-8719/03/$15.
- Mederos, S., Tikoff, B., and Bankey, V., 2005, Geometry, timing, and continuity of the Rock Springs uplift, Wyoming, and Douglas Creek arch, Colorado—implications for uplift mechanisms in the Rocky Mountain foreland, U.S.A.: Rocky Mountain Geology, v. 40, p. 167–191. Mews, K., Mustafa, A.M., and Barati, Rh., 2019, A review of brittleness index correlations for unconventional tight and ultra-tight reservoirs: Geosciences, v. 9, 10.3390/geosciences9070319.
- Morgan, C.D., 2003, Geologic guide and road logs of the Willow Creek, Indian, Soldier Creek, Nine Mile, Gate, and Desolation Canyons, Uinta Basin, Utah: Utah Geological Survey Open-File Report 407, 74 p., https://geology.utah.gov/resources/ energy/oil-gas/green-river-formation-project/.
- Morgan, C.D., McClure, K.P., Bereskin, S.R., and McPherson, M., 2002, A preliminary discussion of fault styles in the southwest Uinta Basin, Utah [abs.]: American Association of Petroleum Geologists, Rocky Mountain Section Meeting Program with Abstracts, https://geology.utah.gov/resources/energy/oil-gas/green-river-formationproject/.
- Osmond, J.C., 1965, Geologic history of the Uinta basin, Utah: American Association of Petroleum Geologists Bulletin, v. 49, n. 11, p. 1957-1973.
- Pederson, J., Karlstrom, K., Sharp, W., and McIntosh, W., 2002, Differential incision of the Grand Canyon related to Quaternary faulting—constraints from U-series and Ar/Ar dating: Geology, v. 30, no. 8, p. 739–742.
- Remy, R., 1992, Stratigraphy of the Eocene part of the Green River Formation in the south- central part of the Uinta Basin, Utah: U.S. Geological Survey Bulletin B 1787-BB, p. BB1–BB69.
- Smith, M.E., Carroll, A.R., and Singer, B.S., 2008, Synoptic reconstruction of a major ancient lake system—Eocene Green River Formation, western United States: Geological Society of America Bulletin, v. 120, no. 1/2, p. 54–84, doi: 10.1130/B26073.1.
- Sprinkel, D.A., 2009, Interim Geologic Map of the Seep Ridge 30' x 60' quadrangle: Utah Geological Survey, Utah Geological Survey Open-File Report 549DM, 3 plates.
- Sprinkel, D.A., 2014, The Uinta Mountains—a tale of two geographies and more: Utah Geological Survey, Survey Notes, v. 46, no. 3, p. 1–4.
- Sprinkel, D.A., 2018, Mysteries of the Uinta Mountains—commonly asked questions and answers: Utah Geological Survey, Survey Notes, v. 50, no. 3, p. 1–3.
- Stone, D.S., 1977, Tectonic history of the Uncompahgre uplift, *in* Veal, H.K. editor, Rocky exploration frontiers of the central and southern Rockies: Rocky Mountain Association of Geologists Guidebook, p. 23–30.
- Töro, B., and Pratt, B.R., 2015, Characteristics and implications of sedimentary deformation features in the Green River Formation (Eocene) in Utah and Colorado, *in* Vanden Berg, M.D., Ressetar, R., and Birgenheier, L.P., editors, Geology of Utah's Uinta Basin and Uinta Mountains: Utah Geological Association Publication 44, p. 371– 422.
- Verbeek, E.R., and Grout, M.A., 1993, Geometry and structural evolution of gilsonite dikes in the eastern Uinta Basin, Utah: U.S. Geological Survey Bulletin 1787-HH, 42 p., 1 plate.
- Wawrzyniec, T.F., Geissman, J.W., Melker, M.D., and Hubbard, M., 2002, Dextral shear along the eastern margin of the Colorado Plateau—a kinematic link between Laramide contraction and Rio Grande rifting (Ca. 75–13 Ma): Journal of Geology, v. 110, p. 305–324.